MAJOR PROJECT REPORT

ON

STUDY AND APPLICATION OF STOCHASTIC GROUND MOTION MODELLING AND SIMULATION

(WITH SEPARABLE TEMPORAL AND SPECTRAL NONSTATIONARITY)

MASTER OF ENGINEERING
IN
CIVIL ENGINEERING
(STRUCTURAL ENGINEERING)

SUPERVISED BY

Shri G.P.AWADHIYA
(Associate Professor)

SUBMITTED BY

VIVEK KUMAR
PANKAJ

DEPARTMENT OF CIVIL & ENVIRONMENTAL ENGINEERING
DELHI COLLEGE OF ENGINEERING
UNIVERSITY OF DELHI
DELHI

CERTIFICATE

This is to certify that this major project report entitled ," STUDY AND APPLICATION OF STOCHASTIC GROUND MOTION MODELLING AND SIMULATION (WITH SEPARABLE TEMPORAL AND SPECTRAL NONSTATIONARITY)" submitted by Mr. VIVEK KUMAR PANKAJ to the Delhi College of Engineering for the award of M.TECH degree is a record of bonafide Research work carried out by him.

This report fulfills the requirements for submission and has attained requisite standard.

G. P. Awadhiya
ASSOCIATE PROFESSOR
Department of Civil & Environ. Engineering
Delhi college of Engineering
Delhi.

❖ ABSTRACT

A fully nonstationary stochastic model for strong earthquake ground motion has been taken for study. The model employs filtering of a discretized white-noise process. Nonstationarity is achieved by modulating the intensity and varying the filter properties in time. The formulation has the important advantage of separating the temporal and spectral nonstationary characteristics of the process, thereby allowing flexibility and ease in modeling and parameter estimation. The model is fitted to target ground motions by matching a set of statistical characteristics, including the mean-square intensity, the cumulative mean number of zero-level up-crossings and a measure of the bandwidth, all expressed as functions of time. Post-processing by a second filter assures zero residual velocity and displacement, and improves the match to response spectral ordinates for long periods. Hence, together with the target accelerogram, they can be considered as realizations of a stochastic ground motion having the characteristics of the earthquake and site, which produced the target motion. Such an ensemble of ground motions would be appropriate for design or assessment of a structure for that particular earthquake. However, in the broader context of PBEE (performance based earthquake engineering) design and analysis associated with the structure, an ensemble of ground motions that represents all possible earthquakes at a site is of interest.

ACKNOWLEDGEMENTS

I wish to express my deep sense of gratitude and appreciation to Shri G.P.Awadhiya, Associate Professor, Department of Civil & Environmental Engineering, Delhi College of Engineering, Delhi for his guidance and invaluable advice throughout this project without which the completion of this project would have not been possible.

I express my sincere gratitude to all faculty members of Civil & Environmental Engineering and the people from library of Delhi College of Engineering, Delhi providing the relevant information when needed during the course of my project work.

I also express my sincere gratitude to Dr. P.C.Ragtah, Director, P.C.Ragtah & Associates, New Delhi to give valuable & inspiring guidance and excellent advice during the course of my studies.

I also express my sincere thanks to Sanaz Rezaeian, Research Structural Engineer, United States Geological Survey (USGS) for providing valuable information during the project.

I would like to sincere thanks to my family and friends without their moral support, it would have been impossible to accomplish the job.

Vivek Kumar Pankaj

CONTENTS

1.4.2 Types of nonstationarities involved

1.4.2.1 Description of spectral nonstationarity
1.4.2.2 Description of temporal nonstationarity

1.4.3 Model parameters

2 LITERATURE REVIEW
(STOCHASTIC MODELLING OF NONSTATIONARY GROUND MOTIONS)

2.1 Model definition.

2.2 Modulated filtered white noise process.

2.3 Fully nonstationary filtered white noise process.

2.4 Characterization of the ground motion process.

3 MATHEMATICAL MODELING OF NONSTATIONARY GROUND MOTION

3.1 Discretization of the nonstationary process.

3.2. Validation of the model

3.2.1 Identification of parameters in the modulating function
3.2.2 Identification of filter parameters.

3.3. Post - processing of the nonstationary process

3.3.1 Description of post-processing
3.3.2 Adjustment factor for zero level up crossings

4. APPLICATIONS

5. NUMERICAL STUDY

5.1 Numerical examples

5.2 Comparison of target and simulated accelerograms.

6. CONCLUSIONS & ANNEXURE

6.**1 Conclusion**

6.2 Annexure

6.2.1 Program listing

7. REFERENCES

1. INTRODUCTION

1. Introduction

- Earthquakes are a source of critical loading condition for structures located in the seismically active region of the earth. A significant feature of the earthquake loading is a large measure of uncertainty associated with the earthquake phenomena. To establish the seismic loading condition for a structure , it is necessary to anticipate the number, size and location of future earthquakes in the region surrounding the site during the service life of the structure. Further, this assessment should be coupled with the prediction of structural response, and damage due to random vibration induced by ground motion of a given intensity. Both these steps involve uncertainty at several stages.The problem is compounded By the fact that potentially damaging strong motion earthquakes occur after long intervals of time and the available data for such events is often statistically insufficient. A probabilistic treatment of earthquake engineering problems, which involves assessment of seismic risk and random vibration analysis, therefore, provides a rational and consistent basis for a seismic design. Accurate response prediction, possibly associated with a measure of confidence in the prediction itself, lies at the core of performance-based earthquake engineering (PBEE). This approach marks a paradigm shift from traditional design and assessment practice, characterised by conservatism and a mostly implicit consideration of uncertainties, to a more transparent, explicit approach.

1.2 CHRACTERISTICS OF EARTHQUAKE GROUND MOTION

1.2.1 Introduction

Most earthquakes of engineering significance are of tectonic origin and are caused by slip along geological faults. While specific source mechanisms leading to a slip vary in different regions of the earth, and are not always fully understood, four basic types of faulting can be identified with strong- motion earthquakes(Housner,1977):

i) low-angle, compressive under-thrust faulting caused by compressive forces generated due to the movement of the sea-floor crustal plate against continental plate;

ii) compressive over-thrust faulting due to shear failure on an inclined fault with the upper portion of the rock moving upward under the action of compressive forces;

iii) extensional faulting on inclined faults due to extensional strains in the earth crust causing rocks overlying the faults to move downwards;

iv) strike-slip faulting which consists of a relative horizontal displacement of the two sides of a fault across an essentially vertical plane.

In most earthquakes the actual slip mechanism is a combination of two, or more, of the above types of faulting. Often slip occurs on an irregular surface and on an more than one fault. The characteristics of the ground motion during an earthquake in the vicinity of the causative fault (near-field) are strongly dependent on the type of faulting and the time history motion of the fault displacement. As we move away from the fault (far-field), the nature of ground motion is primarily determined by the travel path geology. the nature of ground motion at a point on the earth surface is also influenced by the local site conditions that is soil properties and topography.

Characteristics of the source mechanisms, travel-path geology and local site conditions ,therefore determine the nature of ground motion due to an earthquake.

The basic characteristics of the seismic waves depend primarily on : the **stress drop** during the slip; total fault displacement; size of slipped area; roughness of the slipping process; fault shape; and the proximity of the slipped area to the ground surface. As the waves radiate from the fault, they undergo geometric spreading and attenuation due to loss of energy in the rocks. Since the interiors of the earth consists of heterogenous formations, the waves undergo multiple reflections , refractions, dispersions and

attenuations as they travel. The seismic waves arriving at a site on the surface of the earth are a result of complex superposition giving rise to irregular motion which may be modelled as a random vector varying randomly in space and time.

An earthquake causes both translation and rotation at a point on the surface of the earth. For most problems the rotational component can be disregarded , and ground motion treated as a random vector with three orthogonal translation components- two horizontal and one vertical. Each component can be expressed either by an acceleration, velocity or displacement function of time. Although the three forms contain equivalent information and can be derived from each other by differentiation , or integration , it is generally convenient to represent and record earthquake ground motion as acceleration , and derive velocity and displacement through integration , if required. Based on its characteristics, a ground acceleration time-history due to earthquakes may be classified into four broad groups:

i) time-history containing essentially a single shock. Such motions occur at short distances on firm ground during moderate to shallow focus earthquakes. The records exhibit a strong unidirectional character and represent predominantly short period oscillatory motion;

ii) time-history containing moderately long and extremely irregular motion. Such motion occur on firm ground at moderate distances from the focus to large earthquakes. They contain a wide range of frequencies (0.1-30Hz), and generally are of comparable severity in the three directions;

iii) time-history of long duration containing a dominant frequency of vibration. Such motions result from the filtering of the second type of ground motion through layers of soft soil and from successive wave reflections from the mantle; and

v) motions consisting of large- scale , permanent deformation of ground, such as, slides or soil liquefaction.

The actual ground motion during an earthquake may contain the characteristics of two or more, of the type of motions described above.

1.2.2 Parameters describing ground motion:

Ground motion parameters are important for describing the involved characteristics of importance (i.e., amplitude, frequency content, and duration) of strong ground motions.

1.2.2.1 Amplitude parameters

The most common way of describing a ground motion is through the time history.

- Acceleration time history,
- Velocity time history, and
- Displacement time history

Typically, only one of these is recorded directly with the others computed form it by integration/differentiation. Note that integration produces a smoothing or filtering effect. The acceleration time history displays more high frequency content (relatively), the velocity time history displays more intermediate frequency content (relatively), and the displacement displays more low frequency content (relatively).

1.2.2.1.1 Peak acceleration

Peak horizontal acceleration (PHA): the largest (absolute) value of the horizontal acceleration. Because of its relationship to inertial force, intensity-acceleration relationships can be used to estimate PHA when other information is not available. *Peak vertical acceleration (PVA):* the largest (absolute) value of the vertical acceleration. It is often assumed that the ratio of PVA to PHA is 2/3 for engineering purposes, although the ratio is quite variable. Generally, PVA/PHA is greater than 2/3 near the source and less than 2/3 at large distance.

Ground motions with high peak accelerations are usually, but not always, more destructive than motions with lower peak accelerations. Damage is also related to other characteristics (e.g., frequency content and duration).

1.2.2.1.2 Peak velocity

Since the velocity is more sensitive to the intermediate frequency components of the ground motion, the PHV may characterize the ground motion more accurately at intermediate frequencies than the PHA. The PHV may provide a much more accurate indication of the potential for damage in structures that are more sensitive to loading in the intermediate frequency range.

1.2.2.1.3 Peak displacement

Peak displacements are generally associated with the lower-frequency components of a ground motion. They are, however, often difficult to determine accurately due to signal processing errors and long period noise. They are less commonly used than peak acceleration and peak velocity.

1.2.2.1.4 Sustained maximum acceleration and velocity

It is the 3rd or 5th largest peak in an acceleration or velocity time history. Damage, in some cases, may require repeated cycles of high amplitude to develop.

1.2.2.2 Frequency content parameters

1.2.2.2.1 Ground motion spectra

Fourier spectra

Fourier transform brings a motion in the time domain to the frequency domain. Fourier amplitude spectrum is a plot of Fourier amplitude versus frequency, showing the distribution of the amplitude of a motion with respect to frequency. It expresses the frequency content of a motion very clearly. Large earthquakes produce greater low frequency motions than smaller earthquakes. Fourier phase spectrum is a plot of Fourier phase angle versus frequency. It describes the relative variation between the constituent harmonic signals in the motion time history.

Response spectra

The response spectrum describes the maximum response of a SDOF system to a particular input motion as a function of the natural frequency and damping ratio of the SDOF system. It provides information on the potential effects of an input motion on different structures.

 A linear response spectrum corresponds to a linear structural force displacement relationship.
 A nonlinear response spectrum corresponds to a nonlinear structural force displacement relationship.
 Acceleration response spectra: Maximum acceleration response versus structural natural frequency and damping ratio.
 Velocity response spectra: Maximum Velocity response versus structural natural frequency and damping ratio.
 Displacement response spectra: Maximum displacement response versus structural natural frequency and damping ratio.

1.2.2.2.2 Spectral parameters

Predominant period: the period corresponds to the peak Fourier amplitude.
Bandwidth: the range of frequency over which some level of Fourier amplitude is exceeded.

1.2.2.3 Duration

Degradation of stiffness and strength of certain types of structures and the buildup of pore water pressures in loose, saturated sand, are sensitive to the number of cycles of a ground motion. The duration of strong ground motion is related to the time required to release the accumulated strain energy by rupture along the fault. The strong motion duration increases with earthquake magnitude. The most commonly used definition is the bracketed duration. It is defined as the time between the first and last exceedances of a threshold acceleration.

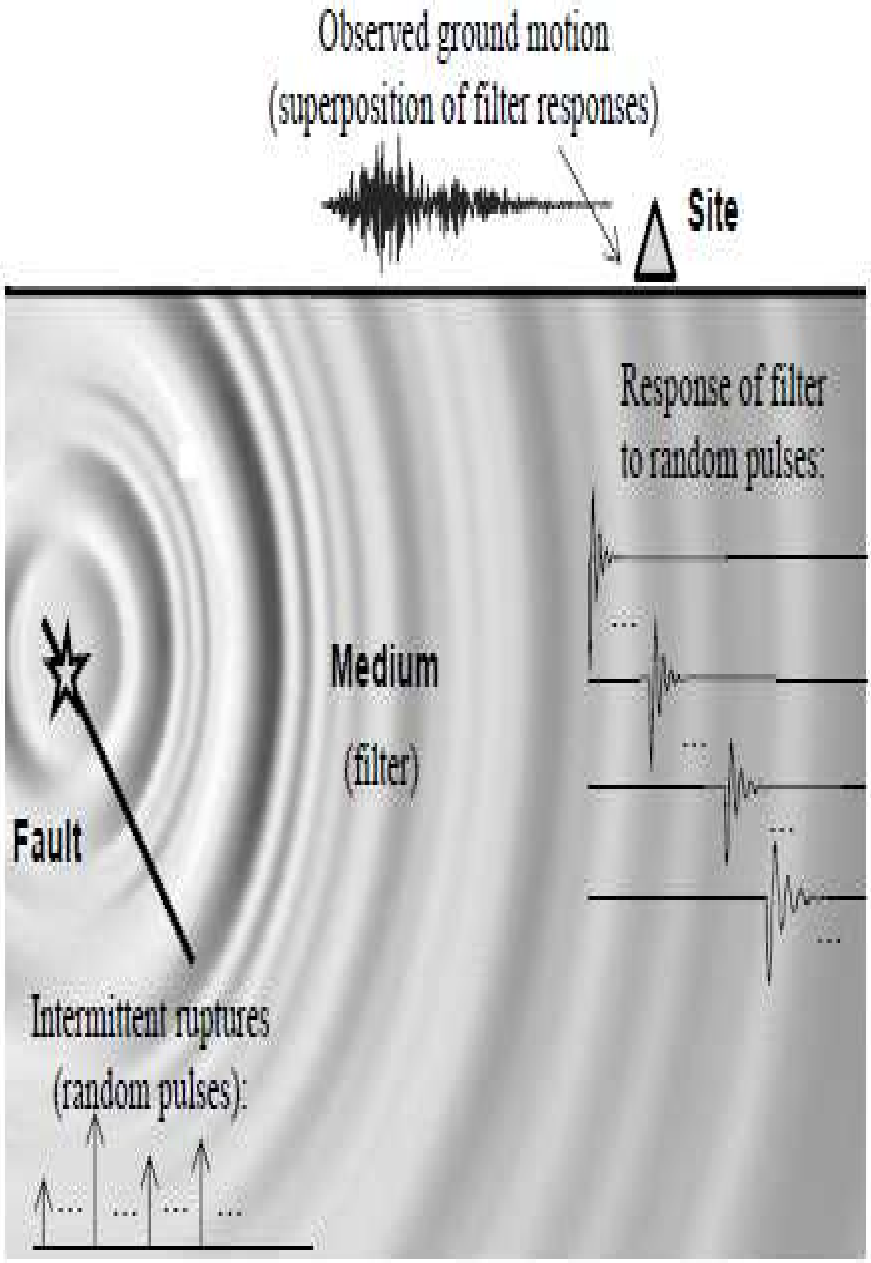

Representation of earthquake excitation as a filtered white-noise process.

1.3. MATHEMATICS INVOLVED IN RANDOM VIBRATIONS:

1.3.1 **Autocorrelation and covariance**:

Let t1 and t2 be two fixed values of t and use the abbreviations x1 and x2 to denote the ensembles of samples x(t1) and x(t2). Let f(x) and g(x) be known functions. We wish to obtain the ensemble average of f(x1).g(x2).

Consider first the experimental case where n sample functions x(j)(t), j==1,…,n, are available. At the fixed times t1 and t2 these provide n pairs of values x1(j) and x2(j). Under the assumption that those n samples are representative of the process, the average of f(x1) g(x2) would be simply

$$\sum_{j=1}^{n} \left(\frac{1}{\mathrm{n}}\right) f(x1^{(j)}) g(x2^{(j)})$$

which can be interpreted as a weighted sum of f(x1) g(x2) values where each weighting factor gives the fraction of sample having that particular f(x1) g(x2) value. The interpretation permits easy generalization to the continuous case where the distribution of x1 and x2 is described by the second-order probability density p(x1, x2). Since the fraction of samples for which x1 lies between x1 and x1 + dx1 and for which x2 lies between x2 and x2 + dx2 is p(x1, x2) dx1 dx2, the ensemble average or mathematical expectation of the product f(x1) g(x2) is

$$E[f(x_1)\, g(x_2)] = \iint_{-\infty}^{\infty} f(x1)\, g(x2)\; p(x1, x2)\, dx1\, dx2 \qquad (1)$$

When f(x1) =x1 and g(x2)= x2 in eq. (1) the resulting average E[x1x2] is called the autocorrelation function.

$$E[x(t1)\, x(t2)] = \iint_{-\infty}^{\infty} x1\, x2\; p(x1, x2)\, dx1\, dx2$$

The prefix auto refers to the fact that x1,x2 represents a product of values in the same sample at two instants. For fixed t1 and t2 this average is simply a constant; however, in subsequent applications t1 and t2 will be permitted to vary and the autocorrelation will in general be a

function of both t1 and t2. In an important special case the autocorrelation function is a function only of $\tau = t1 - t2$.

A related average, the covariance is obtained by averaging the product of the deviations from the means at two instants. Thus we set $f(x1) = x1 - E[x1]$ and $g(x2) = x2 - E[x2]$ in eq. (1) to obtain

$$E[(x1-E[X1])\,(X2 - E[X2])] = \iint_{-\infty}^{\infty} [(x1 - E[X1])\,(X2 - E[X2])\,p(x1, x2)\,dx1\,dx2$$
$$= E[X1X2] - E[X1]\,E[X2]$$

as the covariance.

1.3.2 Stationary Processes

A random process is said to be stationary if its probability distributions are invariant under a shift of the time scale; i.e., the family of probability densities applicable now also applies 10 minutes from or 3 weeks from now. In particular the first-order probability density p(x) becomes a universal distribution independent of time. This implies that all the averages based on p(x) (e.g., the mean E[x] and the variance ...) are constants independent of time. If the second-order probability density p(x1, x2) is to be invariant under a translation of the time scale then it must be a function only of the lag between t1 and t2 and not a function of t1 or t2 individually. Setting $t2 - t1 = \tau$ we can write the second-order density of a stationary process as $p(t, t + \tau)$ and know that it is independent of t. This implies that the autocorrelation function is also a function only of τ.

$$E[X1X2] = E[\,x(t)\,x(t+\tau)] = R(\tau)$$

1.3.3 Temporal Averages:

Given a single sample $x^{(j)}$ of duration t it is, however, possible to obtain averages by averaging with respect to time along the sample. Such an average is called a temporal average in contrast to the ensemble or statistical averages described previously.

Let $x^{(j)} = f(t)$ be a function of time defined from $t = -T/2$ to $t = T/2$. For our purposes it is well to think of f(t) as representing a particular sample of a random process although the following

temporal averages apply to any function f(t) and have nothing to do with random processes, per se. The temporal mean of f(t)

$$< f> = (1/T) \int_{-T/2}^{T/2} f(t)dt$$

and the temporal mean square is

$$< f^2 > = (1/T)\int_{-T/2}^{T/2} f^2(t)\, dt$$

where we have adopted the notation <f> for temporal mean.

1.3.4 Spectral Density of a stationary random process:

Returning now to random processes we recall that for stationary processes the autocorrelation function E[x(t1) x(t2)] was a function R(τ) of the interval τ = t2 – t1. A frequency decomposition of R(τ) can be made in the following way

$$R(\tau) = \int_{-\infty}^{\infty} S(\omega) e^{i\omega\tau} d\tau \qquad (2)$$

where S(ω) is essentially (except for the factor 2..) the Fourier transform of R(τ).

$$S(\omega) = (1/2\pi) \int_{-\infty}^{\infty} R(\tau) e^{-i\omega\tau} d\tau$$

It can be shown [14] that S(ω) is a non-negative, even function of ω.

A physical meaning can be given to S(ω) by considering the limiting case of eq. (2) in which τ =0.

$$R(0) = E[X2] = \int_{-\infty}^{\infty} S(\omega) d\omega$$

The mean square of the process equals the sum over all frequencies of S(ω) dω so that S(ω) can be interpreted as a mean square spectral density.

1.3.5 Wide-Band Processes; White Noise

The terms wide and narrow are qualitative and not precisely delineated. A wide-band process is a stationary random process whose mean square spectral density S(ω) has significant values over a band or range of frequencies which is of roughly the same order of magnitude as the center

frequency of the band. A wide range of frequencies appears in representative sample functions of such a process. Excitation processes which are typically wide-band include the pressure fluctuations on the surface of a rocket missile due to acoustically transmitted jet noise or due to supersonic boundary layer turbulence.

In analytical investigations a common idealization for the spectrum of a wide-range process is the assumption of a uniform spectral density S… as shown. A process with such a spectrum is called white noise in analogy with white light which spans the visible spectrum more or less uniformly. Ideal white noise is supposed to have a uniform density over all frequencies. This is a physically unrealizable concept since the mean square value of such a process would be infinite because there is infinite area under the spectrum. Nevertheless, the ideal white noise model can sometimes be used to provide physically meaningful results in a simple manner.

1.3.6 Duhamel integral:

A force p(t) varying arbitrarily with time can be represented as a sequence of infinitesimally short impulse . the response of a linear dynamic system to one of these impulses , the one at time τ of magnitude $p(\tau)\, d\tau$, is this magnitude times the unit impulse- response function:

$$du(t) = [p(\tau)\, d\tau]\, h(t-\tau) \qquad t > \tau$$

the response of the system at time t is the sum of the responses to all impulses up to that time. Thus,

$$u(t) = \int_o^t p(\tau) h(t-\tau) d\tau \qquad (3)$$

this is known as convolution integral , a general result that applies to any linear dynamic system.

A unit impulse at time $t=\tau$ imparts to the mass m , the velocity

$$u'(t) = 1/m \qquad (4)$$

but the displacement is zero prior to and up to the impulse:

$$u(\tau) = 0 \qquad (5)$$

A unit impulse causes free vibration of the SDF system due to the initial velocity and displacement given by Eqs. (4) and (5) . Substituting these gives the response of undamped system :

$$h(t-\tau) \equiv \quad u(t) = (1/m\omega_n)\sin[\omega_n(t-\tau)] \qquad t \geq \tau$$

similarly, the result for viscously damped systems:

$$h(t-\tau) \equiv \quad u(t) = (1/m\omega_n)\, e^{-\zeta\omega n(t-\tau)} \sin[\omega_D(t-\tau)] \qquad t \geq \tau \qquad (6)$$

Specializing eq. (3) for the SDF system by substituting eq. (6) for the unit impulse response function gives **Duhamel's integral :**

$$u(t) = (1/m\omega_D)\int_0^t p(\tau)\, e^{-\zeta\omega n(t-\tau)} \sin[\omega_D(t-\tau)]d\tau \qquad (7)$$

for an undamped system this result simplifies to

$$u(t) = (1/m\omega_n)\int_0^t p(\tau)\, e^{-\zeta\omega n(t-\tau)} \sin[\omega_n(t-\tau)]d\tau \qquad (8)$$

implicit in this result are "at rest" initial conditions u(0) = 0 and u'(0)=0.

Duhamel integral provides a general result for evaluating the response of a linear SDF system to arbitrary force. This result is restricted to linear systems because it is based on the principle of superposition . thus it does not apply to structures deforming beyond their linearly elastic limit. If $p(\tau)$ is a simple function , closed form evaluation of the integral is possible. Then the Duhamel integral is an alternative to the classical method for solving differential equations.

1.4. NONSTATIONARY PROCESSES

1.4.1 Definition of Nonstationarity process :

A nonstationary process is a stochastic process whose joint probability distribution does change when shifted in time or space. Consequently, parameters such as the mean and variance, if they exist, also change over time or position.

1.4.2 Types of nonstationarities involved：

The following are the types of nonstationarities involved in modeling of ground motions:

i) Spectral Nonstationarity

ii) Temporal Nonstationarity

1.4.2.1 Description of Spectral Nonstationarity :

In the frequency domain, the properties of the model process are influenced by the selection of the filter, i.e., the form of the IRF $h[t-\tau, \lambda(\tau)]$, and its time-varying parameters $\lambda(\tau)$ that are used to "shape" the filter response. In particular, for a second-order filter (employed in this study), the time-varying frequency content of the process may be controlled by the natural frequency and damping of the filter, as they evolve in time. As stated, in choosing the linear filter, certain constraints must be followed to make sure that the choice of the IRF is acceptable:

• The filter should be causal so that $h(t, \lambda)=0$ for $t<0$.

• The filter should be stable so that $\int_0^\infty h(t, \lambda)dt < \infty$ ·

·, which requires $\lim_{t\to\infty} h(t, \lambda)=0$

• The filter must have an IRF that is at least once differentiable so that (25) can be evaluated.

Any damped single or multi-degree-of-freedom linear system that follows the above constraints can be selected as the filter.

In this study, we select

$$h[t-\tau,\boldsymbol{\lambda}(\tau)] = \frac{\omega_f(\tau)}{\sqrt{1-\zeta_f^2(\tau)}}\exp[-\zeta_f(\tau)\omega_f(\tau)(t-\tau)] \times \sin\left[\omega_f(\tau)\sqrt{1-\zeta_f^2(\tau)}(t-\tau)\right];\ \tau \le t$$

$$= 0 \quad \text{otherwise}$$

(9)

which represents the pseudo-acceleration response of a single-degree-of-freedom linear oscillator subjected to a unit impulse, in which τ denotes the time of the pulse and $\lambda(\tau) = [\omega_f(\tau), \zeta_f(\tau)]$ is the set of parameters of the filter with $\omega_f(\tau)$ denoting the natural frequency and $\zeta_f(\tau)$ denoting the damping ratio, both dependent on the time of application of the pulse. We expect $\omega_f(\tau)$ to influence the predominant frequency of the resulting ground motion process, whereas $\zeta_f(\tau)$ to influence its bandwidth.

Aiming for a simple model and based on analysis of a large number of accelerograms, we adopt a linear form for the filter frequency:

$$\omega_f(\tau) = \omega_0 - (\omega_0 - \omega_n)\frac{\tau}{t_n} \qquad (10)$$

In the above expression, t_n is the total duration of the ground motion, ω_n is the filter frequency at time $t_0 = 0$, and ω_n is the frequency at time t_n ▪. Thus, the two parameters ω_0 and ω_n describe the time-varying frequency content of the ground motion. The predominant frequency of a typical earthquake ground motion tends to decay with time; hence, it is expected that $\omega_0 > \omega_n$ for a typical motion. Of course any other two parameters that describe the linear function in (10) may be used in place of ω_0 and ω_n. Investigations of several accelerograms revealed that the variation of their bandwidth measure with time is relatively insignificant. Thus, as a first approximation, the filter damping is considered a constant:

$$\zeta_f(\tau) = \zeta_f \qquad (11)$$

A more refined model for the filter damping ratio that accounts for the observed variation in the bandwidth of some recorded motions can be considered. The refined model is a piece-wise constant function of the form:

$$\zeta_f(\tau) = \begin{cases} \zeta_1 & \text{if } 0 \le \tau \le T_1 \\ \zeta_2 & \text{if } T_1 < \tau \le T_2 \\ \zeta_3 & \text{if } T_2 < \tau \le t_n \end{cases} \quad (12)$$

with parameters ζ_1, ζ_2, ζ_3, T_1, and T_2 that must be identified for a target motion. The function in (12) may have fewer or more than three pieces, as required. One disadvantage of using a single-degree-of-freedom filter, as in (9), is that such a filter can characterize only a single dominant frequency in the ground motion. One can select a multi-degree-of-freedom filter instead to simulate ground motions with multiple dominant frequencies, in which case additional parameters will need to be introduced and identified. This is possible with the proposed model, but is not pursued in the present study.

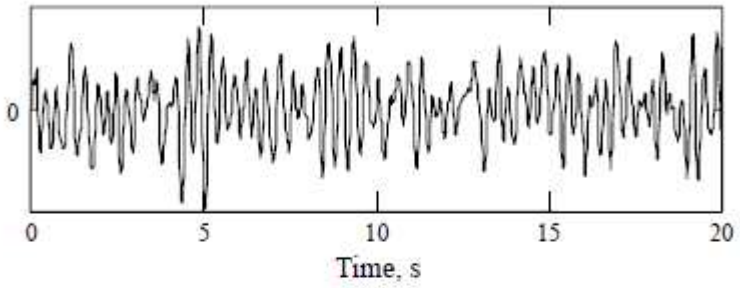

Realization of a stationary filtered white-noise process.

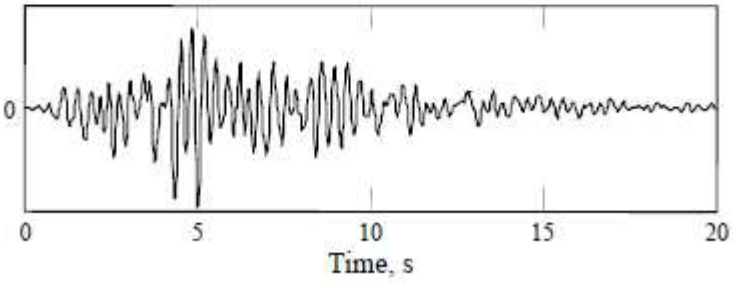

Realization of a time-modulated filtered white-noise process.

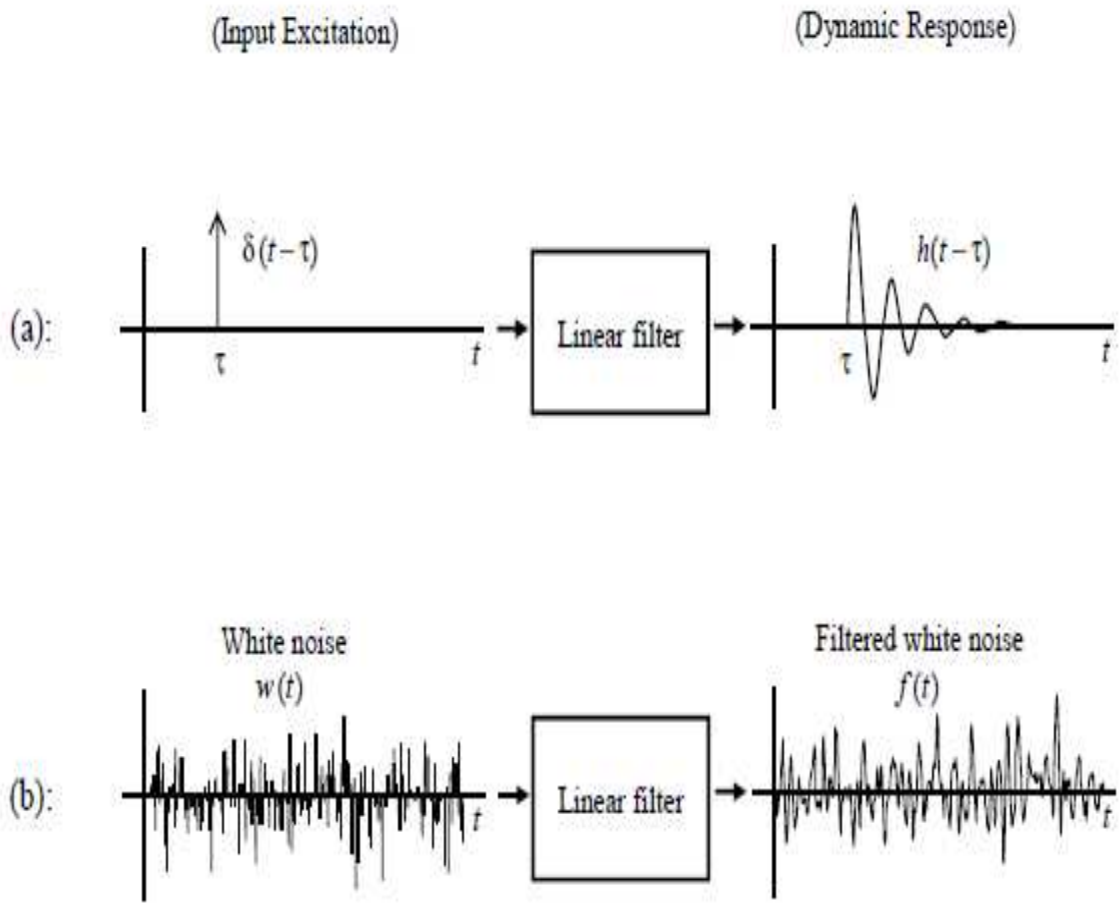

Schematic of input-output relationship for a linear filter. (a) Response of the linear filter to the unit impulse centered at $t = \tau$, indicated by the shifted Dirac delta function $\delta(t - \tau)$, is the impulse response function $h(t - \tau)$. (b) Response of the linear filter to the white-noise excitation, $w(t)$, is the filtered white-noise process, $f(t)$.

1.4.2.2 Description of Temporal Nonstationarity :

In general, any function that gradually increases from zero to achieve a nearly constant intensity that represents the "strong shaking" phase of an earthquake and then gradually decays back to zero is a valid modulating function. Several models have been proposed in the past. These include piece-wise modulating functions proposed by Housner and Jennings (1964) and Amin 29 and Ang (1968), a double-exponential function proposed by Shinozuka and Sato (1967), and a gamma function proposed by Saragoni and Hart (1974). Two modulating functions that are employed in this study are presented below.

Piece-wise modulating function:

A modified version of the Housner and Jennings (1964) model that hereafter will be referred to as the "piece-wise" modulating function is defined by

$$
\begin{aligned}
q(t,\boldsymbol{\alpha}) &= 0 && \text{if} \quad t \le T_0 \\
&= \alpha_1 \left(\frac{t-T_0}{T_1-T_0}\right)^2 && \text{if} \quad T_0 \le t \le T_1 \\
&= \alpha_1 && \text{if} \quad T_1 \le t \le T_2 \\
&= \alpha_1 \exp[-\alpha_2 (t-T_2)^{\alpha_3}] && \text{if} \quad T_2 \le t
\end{aligned}
\qquad (13)
$$

This model has six parameters $T0$, $T1$, $T2$, σ max,α and β, which obey the conditions $T_0 < T_1 \le T_2$, $0 < \sigma$max, $0 < \alpha$ and $0 < \beta$. (The Housner–Jennings model has $\beta = 1$.) $T0$ denotes the start time of the process, T_1 and T_2 denote the start and end times of the strong-motion phase with root mean square (RMS) σ max, and α and β are parameters that shape the decaying end of the modulating function. Figure shows a piece-wise modulating function for selected parameter values.

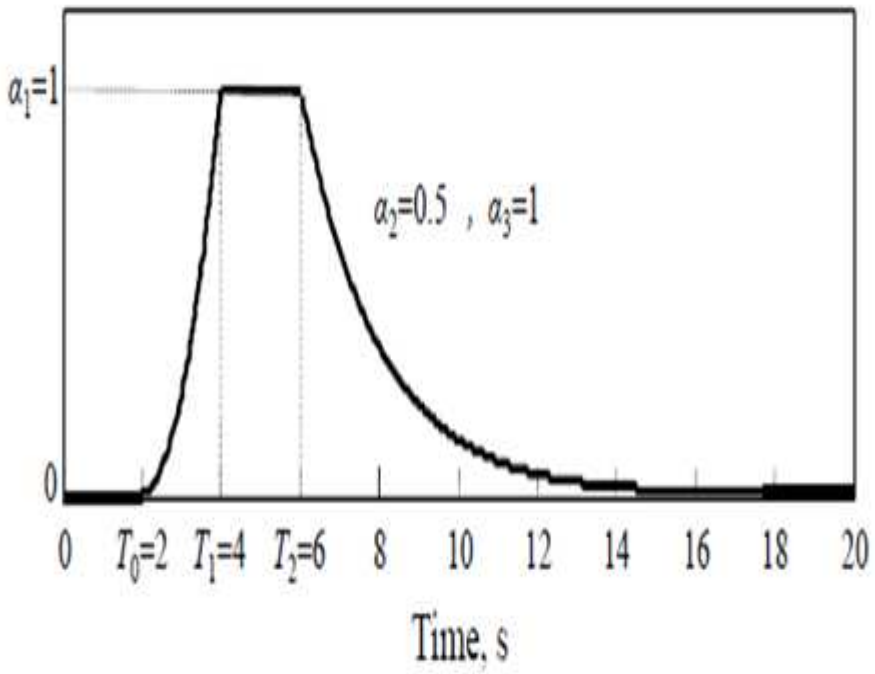

Fig. Piece-wise modulating function for selected parameter values.

Gamma modulating function:

Another model used in this study is the "gamma" modulating function, defined by the formula:

$$q(t,\boldsymbol{\alpha}) = 0 \qquad \text{if} \quad t \le T_0$$
$$= \alpha_1 (t - T_0)^{\alpha_2 - 1} \exp[-\alpha_3 (t - T_0)] \qquad \text{if} \quad T_0 \le t$$

(14)

This function is proportional to the gamma probability density function, thus the reason for its name. The model has four parameters $\alpha = (\alpha_1, \alpha_2, \alpha_3, T_0)$, where $0 < \alpha_1, \alpha_3$, and $1 < \alpha_2$. Again, T_0 denotes the start time of the process. Of the other three parameters, α_1 controls the intensity of the process, α_2 controls the shape of the modulating function, and α_3 controls the duration of the motion. Figure shows a gamma modulating function for selected parameter values.

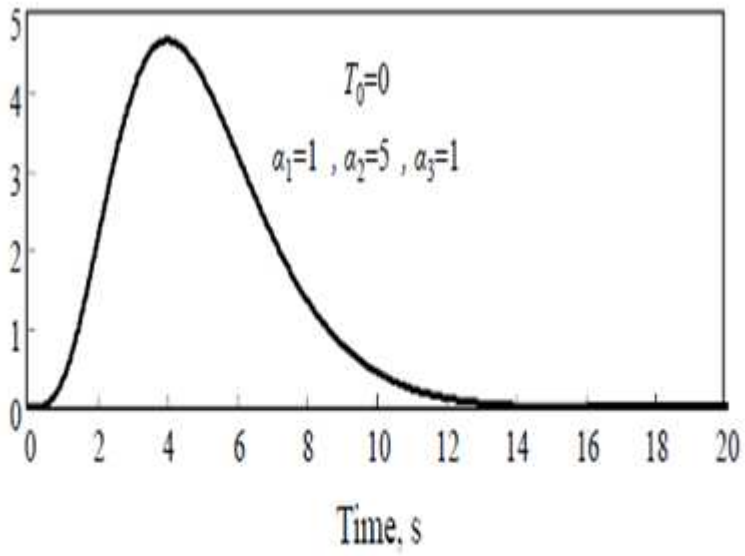

Fig. Gamma modulating function for selected parameter values.

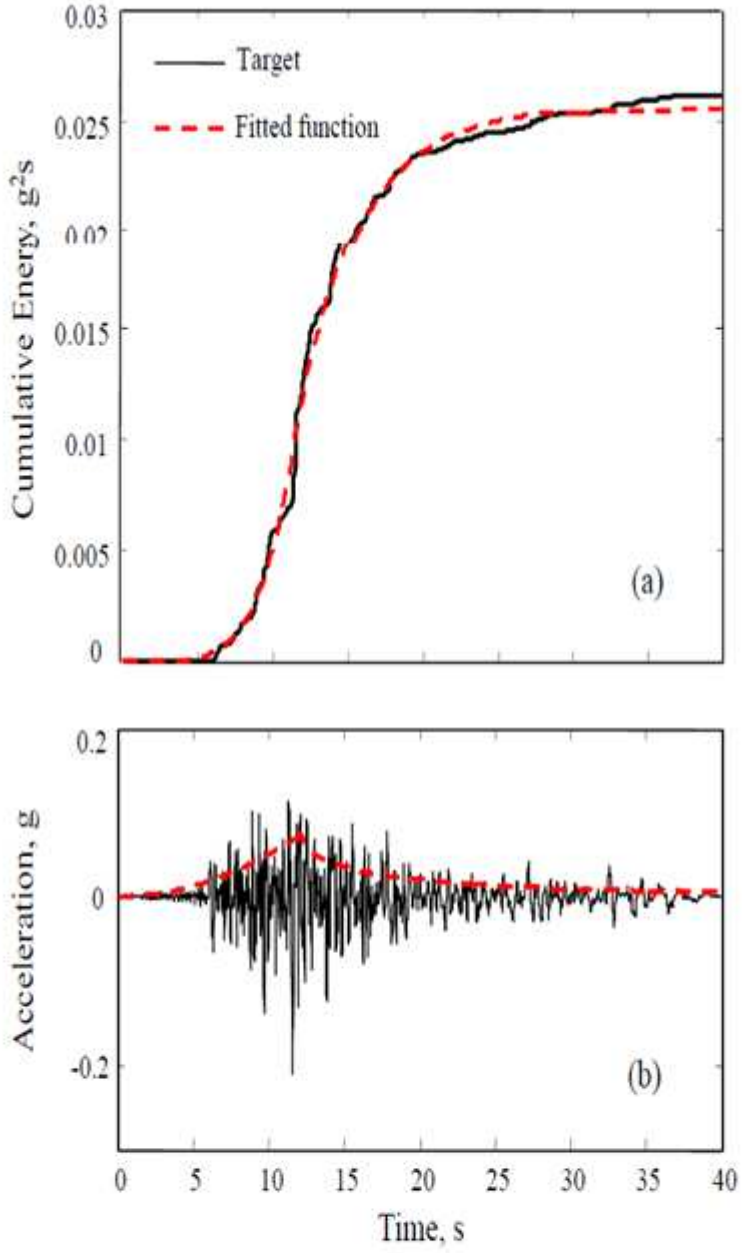

Fig. **(a) Cumulative energies in the target accelerogram and the fitted modulating function. (b) Corresponding modulating function superimposed on the target accelerogram.**

1.4.3 Model Parameters

With the above parameterization, the stochastic ground motion model is completely defined by specifying the forms of the modulating and IRF functions, and the parameters that define them. Specifically, the parameters $\alpha = (\alpha_1, \alpha_2, \alpha_3, T_0, \ldots)$ define the modulating function and completely control the temporal nonstationarity of the process (six parameters (α_1, α_2, α_3, T_0,T_1, T_2) if a "piece-wise" formulation is selected, four parameters (α_1, α_2, α_3, T_0) if a "gamma" formulation is selected). With a linearly varying filter frequency and a constant filter damping ratio, the three parameters (ω_0,ω_n, ζ_f) define the filter IRF and completely control the spectral nonstationarity of the process. Therefore, the total number of the model parameters may be as few as six if $T_0 = 0$ is selected:

(α_1, α_2, α_3 , ω_0, ω_n , ζ_f).

2. LITERATURE REVIEW

2.1. Model Definition:

Stochastic models for characterization and simulation of earthquake ground motions have been of interest for a long time. They are useful in generating artificial samples of ground motions with specified characteristics, which can be used for the evaluation of seismic demand on structures, foundations and soils by time-history dynamic analysis. Stochastic ground motion models are also directly employed for the probabilistic assessment of seismic demand by the random vibration analysis. The growing interest in performance-based earthquake engineering (PBEE) in recent years has further increased the need for stochastic modeling of ground motions. The PBEE analysis typically considers the entire spectrum of structural response, from linear to grossly nonlinear and even collapse [30]. For such an analysis, realistic characterization of the ground motion is essential. In the current PBEE practice (either in research or engineering practice), usually recorded ground motions are employed, which are then scaled to various levels of intensity in order to evaluate fragility curves for structural damage measures [28]. This approach suffers from scarcity of recorded ground motions for specified earthquake characteristics (magnitude, distance, type of faulting, site conditions, etc.), and from concerns regarding the validity of the scaling of recorded motions. Stochastic ground motion models provide an alternative for use in PBEE in lieu of or in conjunction with recorded ground motions.

There are two types of stochastic ground motion models: models that describe the random occurrence of fault ruptures at the source and propagation of the resulting seismic waves through the ground medium (‘source-based’ models, see [19] for a review), and models that describe the ground motion for a specific site by fitting to a recorded motion with known earthquake and site characteristics (‘site-based’ models). Our focus in this paper is on the latter. By using a site based stochastic model, one is able to generate artificial ground motions, which have statistical characteristics similar to those of the target ground motion. By performing such analyses for a large number of recorded ground motions, one may construct correlations between the model parameters and the earthquake and site characteristics (similar to attenuation laws). Such correlations will allow generation of artificial ground motions for given earthquake and site characteristics, which is what one needs in PBEE. This paper deals only with the first of these steps, i.e. the development of a stochastic model and identification of its parameters by fitting to a target accelerogram. In a follow-up study, we intend to develop a large database and evaluate correlations between the model parameters and earthquake and site characteristics.

As we have established that the earthquake ground motions are nonstationary in both time and frequency domains. Temporal nonstationarity refers to the variation in the intensity of the ground motion in time. Spectral nonstationarity refers to the variation in the frequency content of the motion in time.

Although temporal nonstationarity can be easily modeled by multiplying a stationary process by a time function, spectral nonstationarity is not so easy to model. However, both effects are important, particularly in the nonlinear response analysis. Inelastic, degrading structures tend to have resonant frequencies, which decay with time as the structure responds to strong shaking. This trend may coincide with the variation in time of the predominant frequency of the ground motion, thus enhancing the demand [24]. Therefore, realistic representation of the nonstationary characteristics of earthquake ground motions is essential for the PBEE analysis. From a practical standpoint, it is desirable that the model be parsimonious, i.e. have as few parameters as possible. Furthermore, it is helpful if the parameters have physical meaning; hence, one can gain insight from their identification. Finally, it is desirable for the model to have a form, which facilitates the random vibration analysis for linear as well as nonlinear systems.

A large number of site-based stochastic ground motion models have been developed. Formal reviews are presented by Liu [8], Ahmadi [15], Shinozuka and Deodatis [20] and Kozin [21]. The paper by Conte and Peng [26] presents a brief but comprehensive review of more recent work. The existing stochastic models can be classified into four categories: (a) Processes obtained by passing a white noise through a filter (e.g. [1,5,6,7,10]), with subsequent modulation in time to achieve temporal nonstationarity. These processes have essentially time-invariant frequency content. (b) Processes obtained by passing a train of Poisson pulses through a linear filter (e.g. [2, 4]). Through modulation in time, these processes can possess both temporal and spectral nonstationarities [18].

However, matching with recorded ground motions is difficult. (c) Auto-regressive moving average models (e.g. [21,13,14,16,17,25,29]). By allowing themodel parameters to vary with time, thesemodels can have both temporal and spectral nonstationarity. However, it is difficult to relate the model parameters
to any physical aspects of the ground motion. (d) Various forms of spectral representation (e.g. [26, 12,22,31]). The focus in these models is in developing a time-varying spectral representation. These models require extensive processing of the target recorded ground motion. Virtually, all these models assume the ground motion to be a zero-mean Gaussian process.

The stochastic ground motion model developed in this paper is a modulated, filtered Gaussian white-noise process. However, unlike previous models, the filter used in this study has time-varying properties, thus allowing variation of the spectral content with time. Temporal nonstationarity is achieved by modulation in time, as is done in most previous studies. The filter properties are adjusted to capture the time-varying predominant frequency and bandwidth of the target accelerogram.

Two models are particularly relevant to this study. One is the model by Yeh and Wen [23], which is also a Gaussian filtered white-noise process. They use a time-invariant filter; however,

to achieve spectral nonstationarity, they modify the timescale through a nonlinear transformation. The model parameters are identified by matching the cumulative energy and zero-level up-crossings of the target motion. The approach for estimating the model parameters in the present work is similar to that used by Yeh and Wen [23]. The second is a model developed by Papadimitriou [24], which is based on a second-order differential equation with time-varying properties and subjected to a modulated Gaussian white noise (essentially a filtered white-noise process). Papadimitriou derives approximate expressions for the second-moment statistics of the process. This model can be seen as a special case of the model presented in this paper (the filter in the present formulation can be more general). Furthermore, in this study, the approaches to parameterization and fitting of the model are entirely different. In particular, the present model has the important advantage that the temporal and spectral nonstationary characteristics are completely separated, thus facilitating parameter estimation.

Compared with the existing models, the proposed model has the following advantages: (a) the model has a small number of parameters, which control the temporal and spectral nonstationary characteristics of the simulated ground motion and can be easily identified by matching with similar characteristics of the target accelerogram; (b) the temporal and spectral nonstationary characteristics are completely separable, facilitating identification and interpretation of the parameters; (c) there is no need for sophisticated processing of the target accelerogram, such as the Fourier analysis or estimation of evolutionary power spectral density; (d) the filter model provides physical insight and its parameters can be related to the characteristics of the earthquake and site considered; (e) simulation of sample functions is simple and requires little more than generation of standard normal random variables; and (f) the model is of a form, which facilitates nonlinear random vibration analysis by the tail-equivalent linearization method (TELM) [33].

Virtually, all site-based stochastic ground motion models fail to match the response spectrum associated with the target accelerogram in the long-period range (typically greater than 2 s), and the model proposed here is no exception. To make a correction, we post-process the stochastic model by passing it through a filter based on Brune's [9] source model. With such a post-processing, the simulated motion is appropriate for periods as long as 5–10 s.

We begin this paper with a new formulation of the filtered white-noise model, which through a normalization separates the temporal and spectral characteristics of the process. The model is then extended by allowing the filter parameters to vary with time, while maintaining complete separation of the time-varying temporal and spectral characteristics. A discrete representation the process is then developed, whereby the process is defined as the summation of standard normal random variables with time-varying coefficients. This form is of particular interest for the nonlinear random vibration analysis [33]. This is followed by parameterization of the model and description of a method for estimation of the

model parameters. The last section describes simulation of artificial ground motions fitted to a selected accelerogram and its post-processing to correct for long periods.

2.2. Modulated Filtered White Noise Process:

The modulated filtered Gaussian white-noise process is obtained by time modulating the stationary response of a linear filter subjected to a Gaussian white-noise excitation. Let the linear filter be defined by its impulse response function (IRF) $h(t, \boldsymbol{\theta})$, where $\boldsymbol{\theta}$ denotes a set of parameters used to 'shape' the filter response. Specifically, $\boldsymbol{\theta}$ may include the natural frequency and damping of the filter, which control the predominant frequency and bandwidth of the process. We assume that the filter is causal so that $h(t, \boldsymbol{\theta})=0$ for $t<0$, and that it is stable so that $\int_{-\infty}^{\infty} h(t, \boldsymbol{\theta})\mathrm{d}t<\infty$, which also implies $\lim_{t\to\infty} h(t)=0$. We also assume $h(t, \boldsymbol{\theta})$ is at least once differentiable. Note that this requires $h(t, \boldsymbol{\theta})$ to start from a zero value at $t=0$ and not have any discontinuities. The modulated filtered Gaussian white-noise process can be expressed in the form

$$x(t)=q(t)\left[\frac{1}{\sigma_h}\int_{-\infty}^{t} h(t-\tau,\boldsymbol{\theta})w(\tau)\,\mathrm{d}\tau\right] \qquad (15)$$

where $q(t)$ is the (deterministic, non-negative) modulating function, $w(t)$ denotes the Gaussian white-noise process, and σh is the standard deviation of the filtered white-noise process represented by the integral inside the square brackets. Since the response of a stable filter to a white-noise excitation becomes stationary after sufficient time, and since the white-noise process is assumed to have started in the infinite past (the lower limit of the integral is $-\infty$), the filter response at any finite time point is stationary and, therefore, σ_h is a constant. One can easily show that

$$\sigma_h^2=2\pi S\int_{-\infty}^{t} h^2(t-\tau,\boldsymbol{\theta})\,\mathrm{d}\tau \qquad (16)$$

where S is the intensity of the white-noise process. An important advantage of expressing the modulated filtered white-noise process in the form of (9) is that the segment inside the square brackets is a unit-variance stationary process, so that the intensity of the process is solely controlled by the modulating function $q(t)$. In fact, the standard deviation of the process $x(t)$ is

$$\sigma_x(t)=q(t) \qquad (17)$$

Thus, whereas the modulating function $q(t)$ defines the temporal nonstationarity, the normalized process inside the square brackets defines the spectral content of the process, i.e. the time-invariant shape of the power spectral density function. Note that, due to the normalization by σ_h, the intensity of the white-noise process

cancels out and S can be assigned any arbitrary positive value. The modulated filtered white-noise process defined by (9) lacks spectral nonstationarity. That is, the frequency content of the process, as represented by the instantaneous power spectral density, has a time-invariant shape that is scaled in time uniformly over all frequencies according to $q^2(t)$. For this reason, this class of processes are known as being uniformly modulated.

2.3 Fully Nonstationary Filtered White Noise Process :

As mentioned earlier, earthquake ground motions have nonstationary characteristics both in time and frequency domains. The temporal nonstationarity arises from the transient nature of the earthquake event. The intensity of a typical motion gradually increases from zero to achieve a nearly constant intensity during a 'strong shaking' phase, and then gradually decays to zero with a total duration of 20–60 s. The spectral nonstationarity of the ground motion arises from the evolving nature of the seismic waves arriving at a site. Typically, high-frequency (short wavelength) P waves tend to dominate the initial few seconds of the motion. These are followed by moderate-frequency (moderate wavelength) S waves, which tend to dominate the strong-motion phase of the ground motion. Toward the end of the shaking, the ground motion is dominated by low-frequency (long wavelength) surface waves. The complete ground motion is an evolving mixture of these waves with a dominant frequency that tends toward lower values with time. This evolving frequency content of the ground motion can be critical to the response of degrading structures, which have resonant frequencies that also tend to decay with time as the structure responds to the excitation. Thus, in modeling earthquake ground motions, it is crucial that both the temporal and spectral nonstationary characteristics be properly represented. One convenient way to achieve spectral nonstationarity with the filtered white-noise process is to allow the filter parameters to vary with time. Generalizing the form in (15), we define the fully nonstationary filtered white-noise process

$$x(t) = q(t)\left\{\frac{1}{\sigma_h(t)}\int_{-\infty}^{t} h[t-\tau, \boldsymbol{\theta}(\tau)]w(\tau)\,\mathrm{d}\tau\right\} \qquad (18)$$

where the parameters $\boldsymbol{\theta}$ of the filter are now made dependent on the time of application of the load increment. Figure 1 illustrates the idea behind this formulation. The figure shows the responses of the filter to 2 unit load pulses at times τ =1 and 3s, with the filter having a higher frequency at the earlier time. The superposition of such incremental responses to a sequence of random load pulses produces a process that has a time-varying frequency content, as illustrated in Figure 2. Naturally, the response of

such a filter may not reach a stationary state. Therefore, the standard deviation $\sigma_h(t)$ of the process defined by the integral in (18) in general is a function of time. One can easily show that

$$\sigma_h^2(t) = 2\pi S \int_{-\infty}^{t} h^2[t-\tau, \boldsymbol{\theta}(\tau)]\,\mathrm{d}\tau \qquad (19)$$

Owing to the normalization by the standard deviation, the process inside the curved brackets in (12) has unit variance. Hence, the identity in (11) still holds. However, the normalized process inside the curved brackets now has a time-varying frequency content (Figure 2). Thus, whereas the modulating function $q(t)$ completely defines the temporal nonstationarity of the process, the selected filter (the form of the IRF) and its time-varying parameters $\boldsymbol{\theta}(\tau)$ control the spectral nonstationarity of the process. This complete separation of the temporal and spectral nonstationary characteristics of the process offers significant advantage in identifying and interpreting the model parameters, as described below.

The modulating function $q(t)$ used to model ground motions usually starts from a zero value and gradually increases with time. Furthermore, the damping value of the filter used to model ground motions is usually large so that the IRF $h[t-\tau,\boldsymbol{\theta}(\tau)]$ quickly diminishes with increasing.

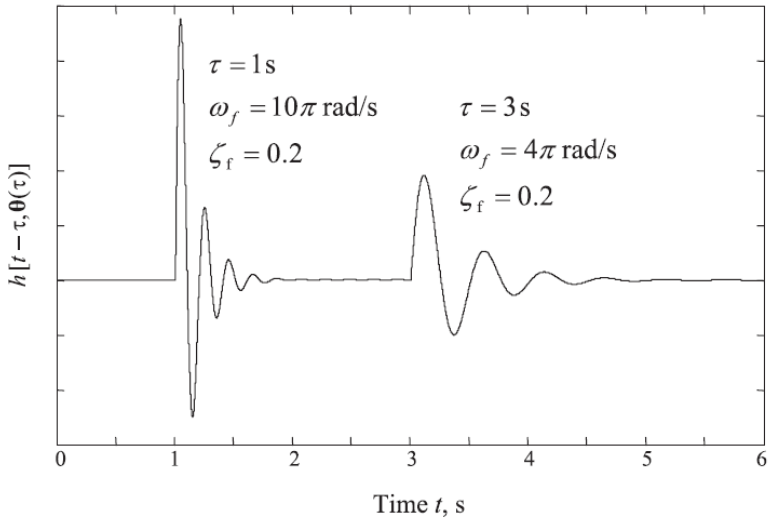

Figure 1. Responses of time-varying filter to unit pulses at two time points.

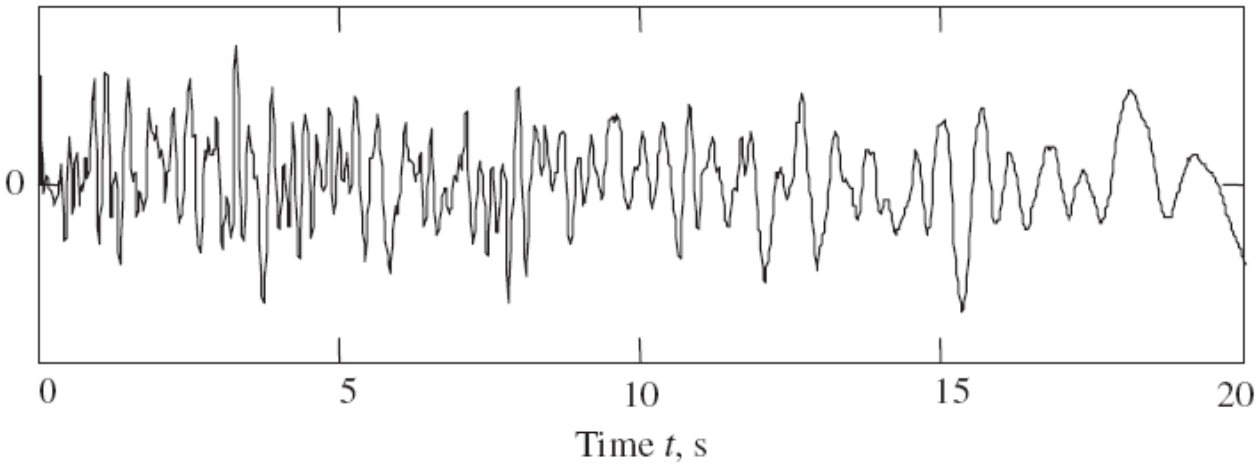

Figure 2. Realization of a constant variance process with time-varying frequency content.

$t-\tau$. Under these conditions, the lower limit of the integral in (18) and (19), which is $-\infty$, can be replaced with zero (or a finite negative value) without much loss of accuracy. This replacement offers a slight computational convenience in the discretization of the process, as described in the following section.

2.4 Characterization of the Ground Motion Process:

The intensity of a zero-mean, Gaussian ground motion process is characterized by its time-varying standard deviation. For the model developed in this paper, this is defined by the modulating function *q(t)*. In the frequency domain, the ground motion process is characterized by a time varying frequency content. In particular, the frequency content may be characterized in terms of a predominant frequency and a measure of the bandwidth of the process, as they evolve in time. These properties of the process are influenced by the selection of the filter, i.e. the form of the IRF $h[t\text{-}\tau,\boldsymbol{\theta}(\tau)]$, and its time-varying parameters $\boldsymbol{\theta}(\tau)$.

As a surrogate for the predominant frequency of the process, we employ the mean zero-level up-crossing rate, $\nu(0+, t)$, i.e. the mean number of times per unit time that the process crosses the level zero from below. Since the scaling of a process does not affect its zero-level crossings, $\nu(0+, t)$ for the process is identical to that for the process

$$y(t)=\sum_{i=1}^{k} s_i(t)u_i, \quad t_k \leqslant t < t_{k+1} \tag{20}$$

It is well known [31] that for such a process

$$v(0^+,t)=\frac{\sqrt{1-\rho_{y\dot{y}}^2(t)}}{2\pi}\frac{\sigma_{\dot{y}}(t)}{\sigma_y(t)} \quad (21)$$

where $\sigma_y(t)$, $\sigma_{\dot{y}}(t)$ and $\rho_{y\dot{y}(t)}$ are the standard deviations and cross-correlation coefficient of $y(t)$ and its time derivative, $\dot{y}(t)=\mathrm{d}y(t)/\mathrm{d}t$, at time t. For the process in (14), these are given by

$$\sigma_y^2(t)=\sum_{i=1}^{k}s_i^2(t)=1, \quad t_k\leqslant t<t_{k+1} \quad (22)$$

$$\sigma_{\dot{y}}^2(t)=\sum_{i=1}^{k}\dot{s}_i^2(t), \quad t_k\leqslant t<t_{k+1} \quad (23)$$

$$\rho_{y\dot{y}}(t)=\frac{1}{\sigma_y(t)\sigma_{\dot{y}}(t)}\sum_{i=1}^{k}s_i(t)\dot{s}_i(t), \quad t_k\leqslant t<t_{k+1} \quad (24)$$

Where $\dot{s}_i(t)=\mathrm{d}s_i(t)/\mathrm{d}t$. Using (12) and $h_i(t)=h[t-t_i,\boldsymbol{\theta}(t_i)]$, one can easily show that

$$\dot{s}_i(t)=\left[\dot{h}_i(t)-\frac{\sum_{j=1}^{k}h_j(t)\dot{h}_j(t)}{\sum_{j=1}^{k}h_j^2(t)}h_i(t)\right]\frac{1}{\sqrt{\sum_{j=1}^{k}h_j^2(t)}}, \quad t_k\leqslant t<t_{k+1}, \quad 0<i\leqslant k \quad (25)$$

It is clear that the filter should be selected so that its IRF is differentiable at all times. Thus, for any given differentiable IRF and filter parameter functions, the mean zero-level up-crossing rate of the process can be computed from (21) by use of the relations in (22)–(25). Naturally, one can expect

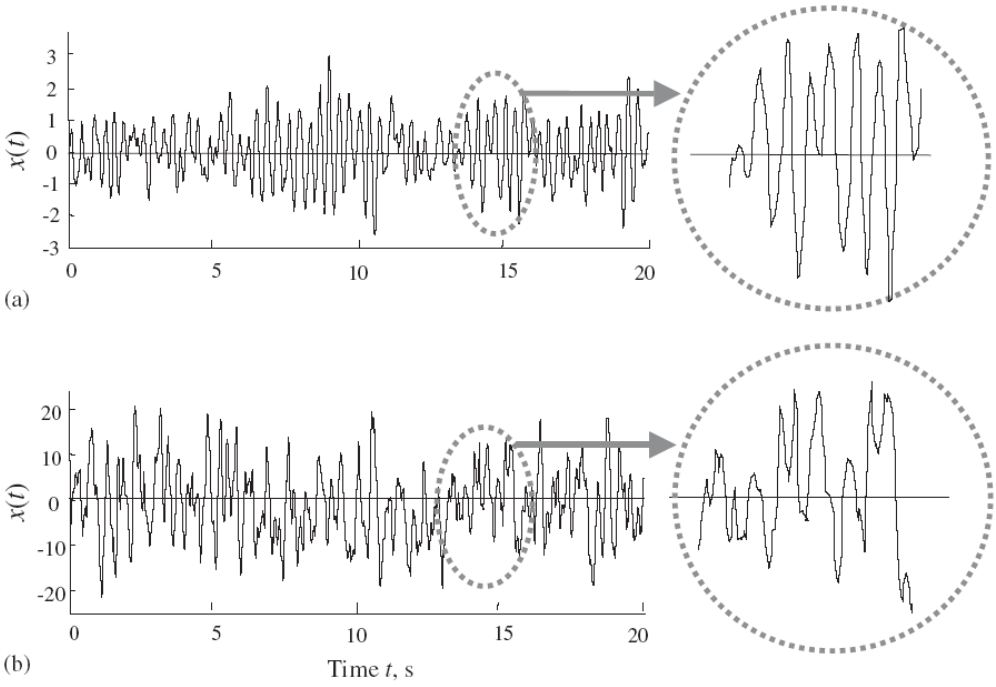

Figure 3. Segments of (a) narrow-band process and (b) wide-band process. Observe the larger number of negative maxima and positive minima in the wide-band process.

that the fundamental frequency of the filter will have a dominant influence on the predominant frequency of the resulting process.

Several alternatives are available for characterizing the time-varying bandwidth of the process. In this paper we use the rate of negative maxima or positive minima as a surrogate for the bandwidth. This measure has the advantage that it is not affected by the modulating function. As is well known, in a zero-mean narrow band process, almost all maxima are positive and almost all minima are negative (see Figure 3(a)). With increasing bandwidth, the rate of occurrence of negative maxima or positive minima increases (see Figure 3(b)). Thus, by determining the rate of negative maxima or positive minima, a time-varying measure of bandwidth can be developed. An analytical expression of this rate for the theoretical model can be derived in terms of the well-known distribution of local peaks [31]. However, the resulting expression is cumbersome, since it involves the variances and cross-correlations of $y(t)$, $\dot{y}(t)$ and $\ddot{y}(t)$ and, therefore, the second derivative of $s_i(t)$. For this reason, in this paper, the rate of negative maxima or positive minima for a selected model process is computed by counting and averaging them in a small sample of simulations (typically 10) of the process. As we will shortly see, the damping of the filter, ζ_f has the dominant influence on the bandwidth of the process.

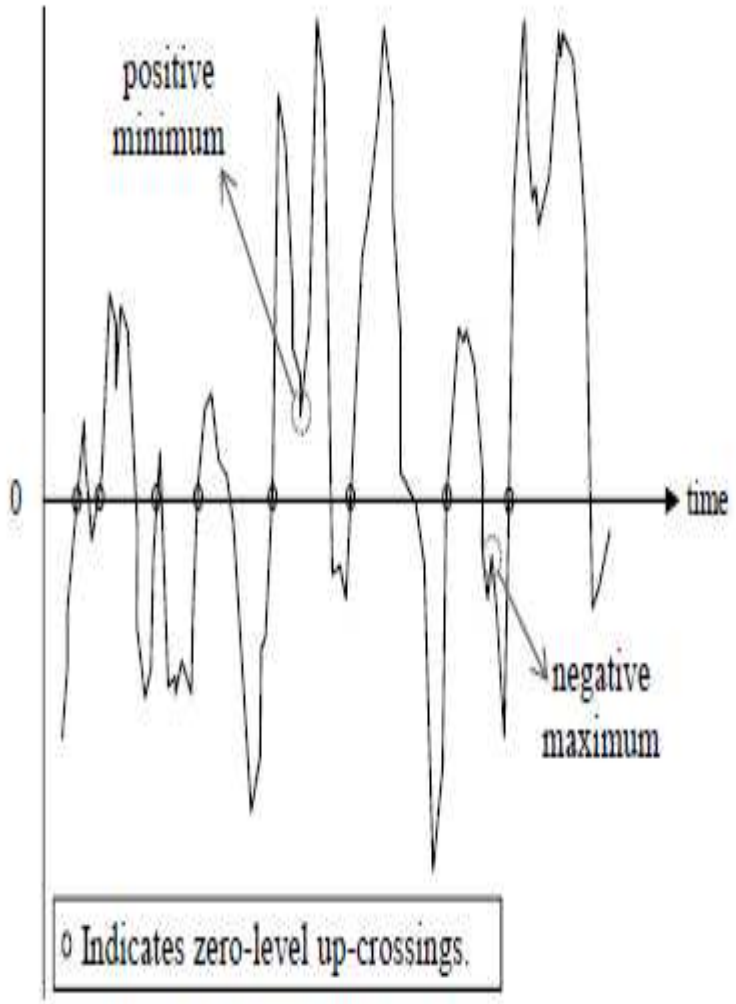

Sample stochastic process, showing zero-level up-crossings, positive minima, and negative maxima.

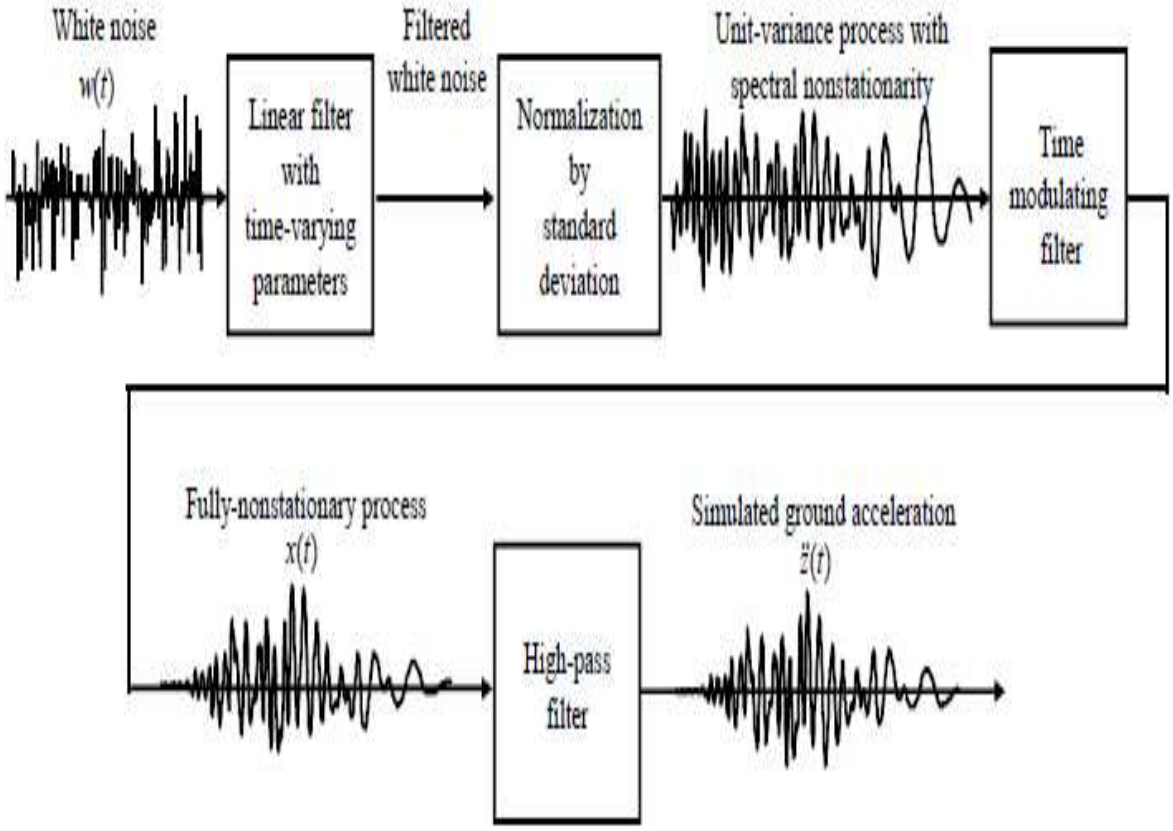

Procedure for generating a single realization of the ground acceleration process according to the proposed model.

THE GROUND MOTION MODEL CAN BE REPRESENTED SCHEMATICALLY AS BELOW:

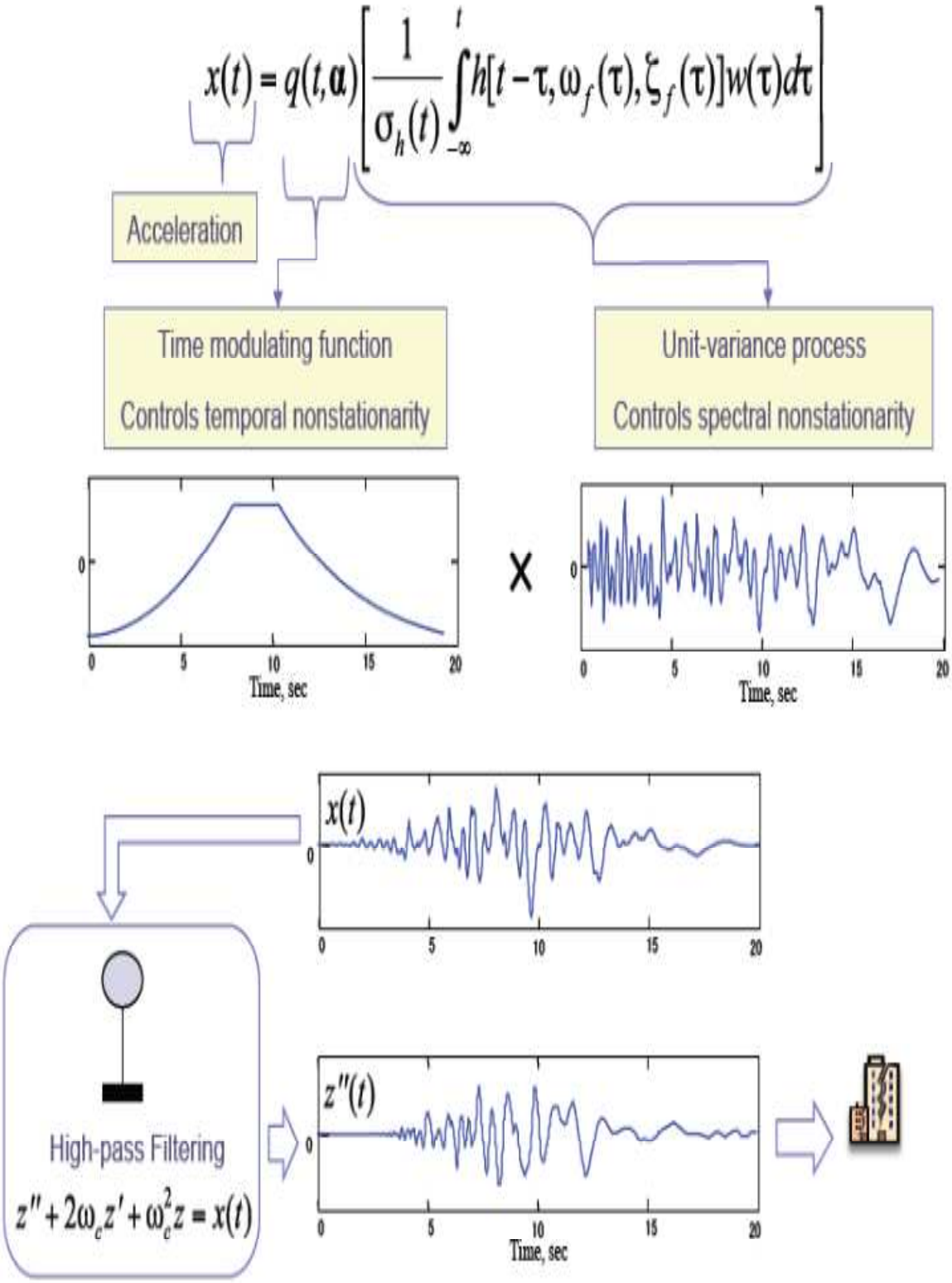

3. MATHEMATICAL MODELLING OF NONSTATIONARY GROUND MOTION

3.1 Discretization of the Nonstationary Process:

We define the fully nonstationary filtered white-noise process

$$x(t)=q(t)\left\{\frac{1}{\sigma_h(t)}\int_{-\infty}^{t}h[t-\tau,\boldsymbol{\theta}(\tau)]w(\tau)\,\mathrm{d}\tau\right\} \qquad (26)$$

where the parameters $\boldsymbol{\theta}$ of the filter are now made dependent on the time of application of the load increment.

In order to digitally simulate a stochastic process, some sort of discretization is necessary. Here, we select a discretization in the time domain. Let the duration of the ground motion be discretized into a sequence of equally spaced time points $t_i = i\times\Delta t$ for $i = 0, 1, \ldots, n$, where Δt is a small time step. At a time t, $0<t\leq t_n$, letting int $(t/\Delta t)=k$, where $0\leq k\leq n$, the process in (26) can be expressed as

$$x(t)=q(t)\left[\frac{1}{\sigma_h(t)}\sum_{i=1}^{k}\int_{t_{i-1}}^{t_i}h[t-\tau,\boldsymbol{\theta}(\tau)]w(\tau)\,\mathrm{d}\tau+\frac{1}{\sigma_h(t)}\int_{t_k}^{t}h[t-\tau,\boldsymbol{\theta}(\tau)]w(\tau)\,\mathrm{d}\tau\right] \qquad (27)$$

Assuming $h[t-\tau,\boldsymbol{\theta}(\tau)]$ remains essentially constant during each small time interval $t_i-1\leq t\leq t_i$ and neglecting the last term, which is an integral over a fraction of the small time step, one obtains

$$\begin{aligned}\hat{x}(t)&=q(t)\left[\frac{1}{\hat{\sigma}_h(t)}\sum_{i=1}^{k}h[t-t_i,\boldsymbol{\theta}(t_i)]\int_{t_{i-1}}^{t_i}w(\tau)\,\mathrm{d}\tau\right]\\&=q(t)\left[\frac{1}{\hat{\sigma}_h(t)}\sum_{i=1}^{k}h[t-t_i,\boldsymbol{\theta}(t_i)]W_i\right],\quad t_k\leqslant t<t_{k+1}\end{aligned} \qquad (28)$$

Where

$$W_i=\int_{t_{i-1}}^{t_i}w(\tau)\,\mathrm{d}\tau \qquad (29)$$

It is easy to show that W_i for all i are statistically independent and identically distributed Gaussian random variables having zero mean and the variance $2\pi S\Delta t$. Introducing the standard normal random variables $u_i = Wi/\sqrt{2\pi S\Delta t}$, (28) can be expressed as

$$\hat{x}(t)=q(t)\left[\frac{\sqrt{2\pi S\Delta t}}{\hat{\sigma}_h(t)}\sum_{i=1}^{k}h[t-t_i,\boldsymbol{\theta}(t_i)]u_i\right],\quad t_k\leqslant t<t_{k+1} \qquad (30)$$

We have superposed hats on two terms in the above expression. The one on $\hat{x}(t)$ is to highlight the fact that expressions (28) and (30) are for the discretized process and employ the approximations involved in going from (27) to (28). The hat on $\hat{\sigma}_h(t)$ is used to signify that this function is the standard deviation of the discretized process represented by the sum inside the square brackets in (28), so that the process inside the square brackets in (30) is properly normalized. Since W_i in (28) are statistically independent random variables, one has

$$\hat{\sigma}_h^2(t) = 2\pi S \Delta t \sum_{i=1}^{k} h^2[t - t_i, \boldsymbol{\theta}(t_i)], \quad t_k \leqslant t < t_{k+1} \tag{31}$$

This equation is the discretized form of (13).

The representation in (30) has the simple form

$$\hat{x}(t) = q(t) \sum_{i=1}^{k} s_i(t) u_i, \quad t_k \leqslant t < t_{k+1} \tag{32}$$

Where

$$\begin{aligned} s_i(t) &= \frac{\sqrt{2\pi S \Delta t}}{\hat{\sigma}_h(t)} h[t - t_i, \boldsymbol{\theta}(t_i)] \\ &= \frac{h[t - t_i, \boldsymbol{\theta}(t_i)]}{\sqrt{\sum_{j=1}^{k} h^2[t - t_j, \boldsymbol{\theta}(t_j)]}}, \quad t_k \leqslant t < t_{k+1}, \ \ 0 < i \leqslant k \end{aligned} \tag{33}$$

The form in (32) has interesting geometric interpretations [27]. In particular, the zero-mean Gaussian process $\hat{x}(t)$ can be seen as the scalar product of a deterministic, time-varying vector of magnitude $q(t)$ along the unit vector $\mathbf{s}(t_k) = [s_1(t_k) \ldots s_k(t_k)]^T$, and a time-invariant, standard normal random vector $\mathbf{u} = [u_1 \ldots u_k]^T$. Furthermore, this representation of the excitation process can be used for nonlinear random vibration analysis by use of the TELM, as described by Fujimura and Der Kiureghian [33].

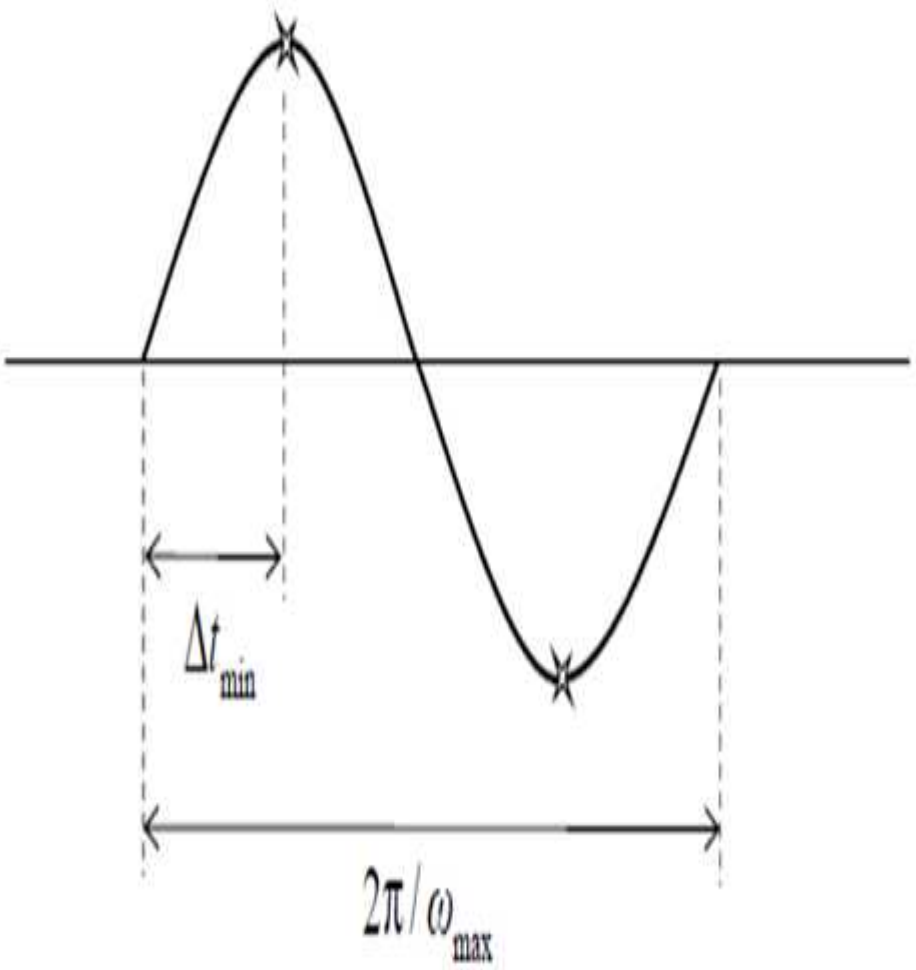

Fig. Minimum acceptable discretization step, Δt.

3.2. VALIDATION OF THE MODEL:

As shown above, the temporal and spectral characteristics of the proposed model are completely separable. Specifically, the modulating function $q(t)$ describes the evolving RMS of the process, whereas the filter IRF $h[t-\tau,\boldsymbol{\theta}(\tau)]$ controls the evolving frequency content of the process. This means that the parameters of the modulating function and of the filter can be independently identified by matching to corresponding statistical characteristics of a target accelerogram.

3.2.1 Identification of parameters in the modulating function

Let $\boldsymbol{\alpha}=(T_0, T_1, T_2, \sigma_{\max}, \alpha, \beta)$ denote the parameters of the modulating function, so that $q(t)= q(t,\boldsymbol{\alpha})$. For a target accelerogram, $a(t)$, we determine $\boldsymbol{\alpha}$ by matching the expected cumulative energy of the process, $Ex(t)=(1/2)\int_o^t q^2(\tau,\boldsymbol{\alpha})\mathrm{d}\tau$, with the cumulative energy in the accelerogram, $Ea(t)= (1/2) \int_o^t a^2(\tau)\mathrm{d}\tau$, over the duration of the ground motion, $0<t \le tn$. This is done by minimizing the integrated squared difference between the two cumulative energy terms, i.e.

$$\hat{\boldsymbol{\alpha}} = \arg\min_{\boldsymbol{\alpha}} \int_0^{t_n} \left[\int_0^t q^2(\tau,\boldsymbol{\alpha}) B(\tau)\,\mathrm{d}\tau - \int_0^t a^2(\tau) B(\tau)\,\mathrm{d}\tau \right]^2 \mathrm{d}t \qquad (34)$$

where $B(t)$ is a weight function introduced to avoid dominance by the strong-motion phase of the record. (Otherwise, the tail of the record is not well fitted.) We have found the function $B(t)=\min\{[\max t\ q_0^2(t)]/q_0^2(t), 5\}$, where $q_0(t)$ is the modulating function obtained in a prior optimization without the weight function, to work well. The objective function in (34), which was earlier used by Yeh and Wen [27] without the weight function, has the advantage that the integral $\int_o^t a^2(\tau)B(\tau)\,\mathrm{d}\tau$ is a relatively smooth function so that no artificial smoothing is necessary.

As an example, Figure compares the two energy terms $2Ex(t)$ and $2Ea(t)$ when fitting to component 090 of the accelerogram recorded at the 116th Street School station during the 1994 Northridge earthquake. The parameter values are T_0=0.0004s, T_1=T_2=12.2s, α =0.413s−1, β =0.552 and

$\sigma_{\max}$=0.0744g. It can be seen that the fit is excellent at all time points. We use this record to illustrate further steps of the parameter identification process. As a measure of the error in fitting to the cumulative energy of the accelerogram, we use the ratio

$$\varepsilon_q = \frac{\int_0^{t_n} |E_x(t) - E_a(t)|\,\mathrm{d}t}{\int_0^{t_n} E_a(t)\,\mathrm{d}t} \qquad (35)$$

The numerator is the absolute area between the two cumulative energy curves and the denominator is the area underneath the energy curve of the target accelerogram. For the example shown in Figure, εq =0.0248.

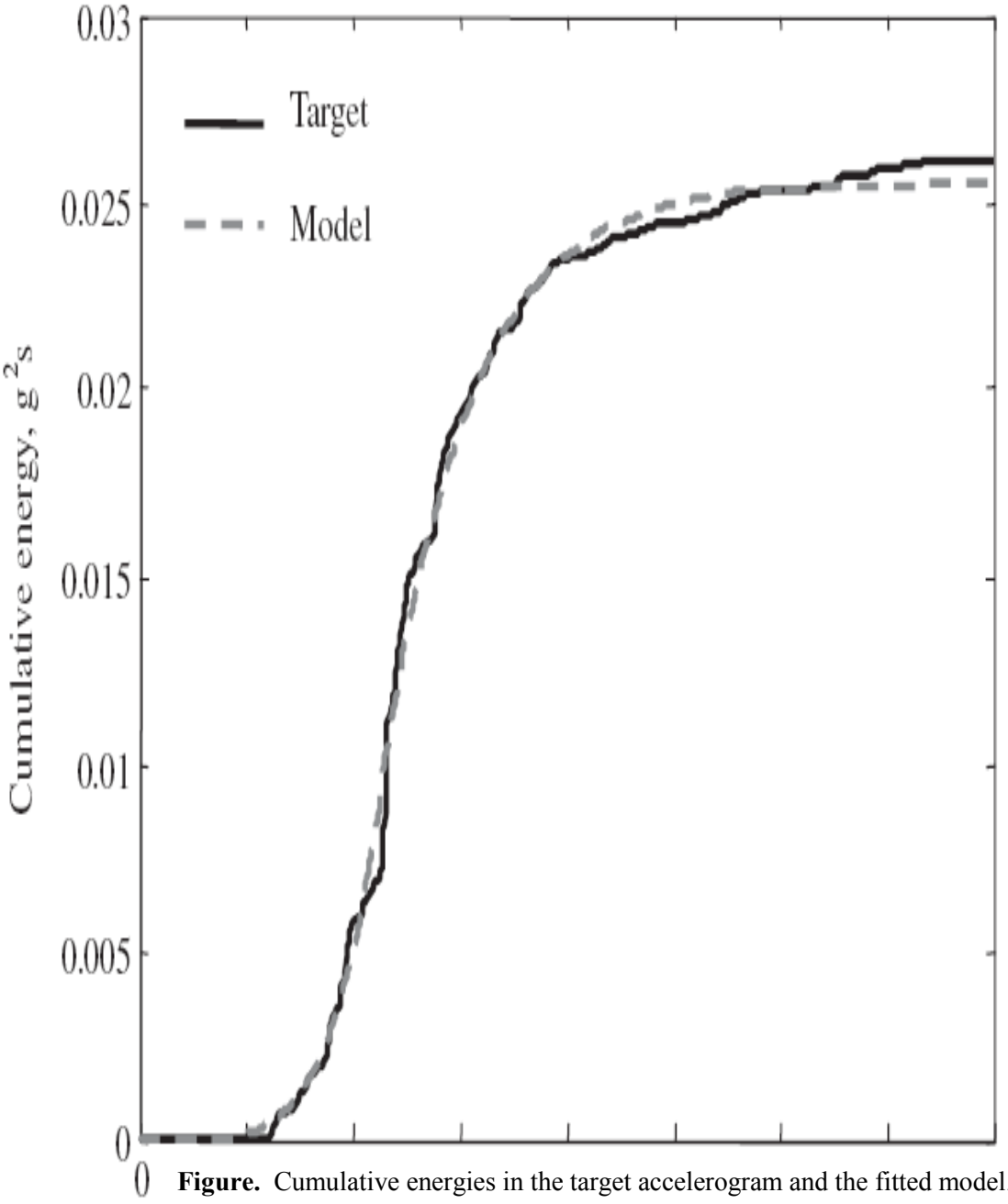

Figure. Cumulative energies in the target accelerogram and the fitted model.

3.2.2 Identification of filter parameters

The parameters $\omega 0$ and ωn defining the time-varying frequency of the filter (see (21)) and parameters defining its damping ratio $\zeta_f(\tau)$ control the predominant frequency and bandwidth of the process. Since these parameters have interacting influences, we first determine ω_0 and ω_n, while keeping the filter damping a constant ζ_f For a given ζ_f , the parameters ω_0 and ωn are identified by matching the cumulative expected number of zero-level up-crossings of the process, i.e. $\int_o^t \nu(0+,\tau)d\tau$, with the cumulative count $N(0+, t)$ of zero-level up-crossings in the target accelerogram for all t, $0<t \le t_n$. This is accomplished by minimizing the mean-square error

$$[\hat{\omega}_0(\zeta_f), \hat{\omega}_n(\zeta_f)] = \arg \min_{\omega_0, \omega_n} \int_0^{t_n} \left[\int_0^t \nu(0^+, \tau) r(\tau)\, d\tau - N(0^+, t) \right]^2 dt \qquad (36)$$

where $r(\tau)$ is an adjustment factor as described below. As can be noted in the equations leading to (15), $\nu(0+,\tau)$ is an implicit function of the filter characteristics $\omega f(\tau)$ and $\zeta_f(\tau)$, and therefore, $\omega 0$, ω_n and ζ_f . The same is true for $r(\tau)$.

When a continuous-parameter stochastic process is represented as a sequence of discrete-time points of equal intervals Δt, the process effectively loses its content beyond a frequency approximately equal to $\pi/(2\Delta t)$ rad/s. This truncation of high-frequency components results in undercounting of level crossings. One can show that the undercount per unit time, denoted r, is a function of Δt as well as the frequency characteristics of the process. In Appendix A, approximate expressions for r are given as functions of Δt, ωf and ζ_f . In the present case, since ω_f is a function of τ, r is also a function of τ.

Since digitally recorded accelerograms are available only in the discretized form, the count $N(0+, t)$ underestimates the true number of crossings of the target accelerogram by the factor $r(\tau)$ per unit time. Hence, to account for this effect, we must multiply the rate of counted up-crossings by the factor $1/r(\tau)$. However, $r(\tau)$ depends on the predominant frequency and bandwidth of the accelerogram. For this reason, it is more convenient to adjust the theoretical mean up-crossing rate (the first term inside the square brackets in (36)) by multiplying it by the factor $r(\tau)$. It is noted that, depending on the time step and filter frequency and damping, the undercount in the rate of up-crossings can be as much as 15% (see Appendix A).

In order to solve (36), we need to select the filter damping ratio, ζ_f , which controls the bandwidth

of the process. As mentioned earlier, we employ a simulation approach to estimate the average cumulative number of negative maxima and positive minima, which characterizes the bandwidth of the model process. Shown in Figure 5 is the cumulative number of negative maxima plus positive minima as a function of time for the Northridge record (thick solid line), as well as the estimated averages of the same quantity for sets of 10 simulations of the theoretical model with damping values ζ_f =0.2, 0.3, 0.4, 0.5, 0.6 and 0.7 (thin solid lines). The slopes of these lines should be regarded as instantaneous measures of bandwidth. The parameters $\hat{\omega}0$ and $\hat{\omega}\, n$ for each value of ζ_f are determined as described above and listed in Table I. Note that the modulating function has no effect on this calculation.

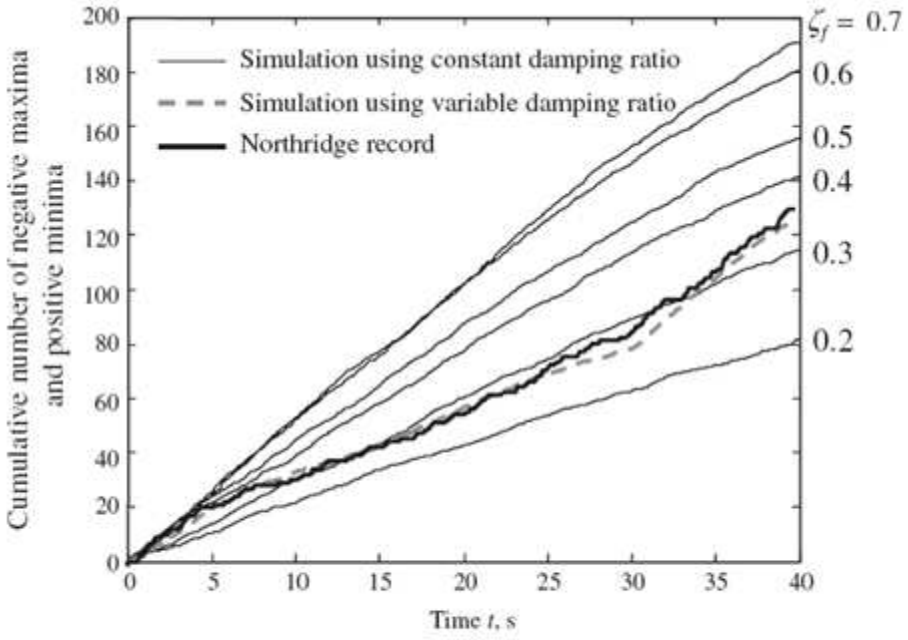

Figure Cumulative count of negative maxima and positive minima.

Table I. Parameter values and error measures.

Damping ratio	Frequency parameters (rad/s)		Error measures	
ζ_f	$\hat{\omega}_0$	$\hat{\omega}_n$	ε_ω	ε_ζ
0.2	40.8	4.16	0.0169	0.3212
0.3	39.7	4.68	0.0167	0.0858
0.4	38.6	4.49	0.0166	0.1925
0.5	38.0	4.55	0.0165	0.2949
0.6	37.4	4.56	0.0166	0.3649
0.7	36.9	4.53	0.0168	0.4004
0.8	36.6	4.46	0.0171	0.4589
0.9	36.3	4.36	0.0174	0.5060
Variable	39.4	4.86	0.0127	0.0461

Several observations in Figure are noteworthy. First, note that the curves based on the theoretical model for the various values of ζ_f are nearly straight lines. This implies that a constant value of the filter damping ratio corresponds to a constant bandwidth of the process, even though the predominant frequency varies with time. This also implies that the bandwidth of the model process is solely controlled by the damping ratio of the filter. Secondly, observe that the curve based on the target accelerogram shows relatively small curvatures. This implies that the bandwidth of this particular accelerogram, as measured in terms of the rate of negative maxima and positive minima, remains more or less constant during the excitation. It can be seen that the theoretical curve with ζf =0.3 best matches the bandwidth of the target accelerogram. If we select ζf =0.3, the corresponding values of the frequency parameters are ω_0=39.7rad/s and $\hat{\omega}n$=4.68rad/s (Table I). These parameter values, together with the parameters identified for the modulating function, completely define the theoretical model fitted to the target accelerogram.

Closer examination of the target curve in Figure shows that the rate of occurrence of negative maxima and positive minima in the Northridge accelerogram is higher during the initial 8 s and final 10 s of the motion relative to the 22 s middle segment. This phenomenon was observed to varying degrees in other accelerograms that were investigated. It appears that ground motions typically have broader bandwidths during their initial and final phases, as compared to their middle segments. This phenomenon may be attributed to mixing of wave forms: In the initial segment, P and S waves are mixed providing a broad bandwidth, the middle segment is dominated by S waves and, therefore, has a narrower bandwidth, whereas the final segment is a mixture of S waves and surface waves, again providing a broader bandwidth.

To more accurately model the time-varying bandwidth of the accelerogram, the filter damping ratio can be made as a function of time. To capture the three-segment behaviour described above, we select three values of the damping ratio for the initial, middle and final segments of the ground motion.

The dashed line in Figure 5 shows the average cumulative number of negative maxima and positive minima for 10 simulations of the fitted model with the filter damping ratio $\zeta_f(\tau)$=0.4 for $0<\tau\leq$8s, (τ)=0.2 for $8<\tau\leq$30s and ζ_f (τ)=0.9 for $30<\tau\leq$40s. These values were selected by comparing the slopes of the observed curve (the thick line in Figure 5) with those of the theoretical curves for different damping ratios (thin lines in the same figure). The corresponding optimal values of the filter parameters (obtained by using the variable damping values in (24)) are $\hat{\omega}_0$=39.4rad/s and $\hat{\omega}_n$=4.86rad/s. It can be seen in Figure 5 that the refined model achieves a close fit to the time-varying bandwidth of the target accelerogram.

Figure 6 compares the cumulative number of zero-level up-crossings of the Northridge accelerogram and the adjusted (by factor $r(\tau)$) mean cumulative number of zero-level up-crossings of the fitted model process with variable filter damping. It is evident that the rate of up-crossings (the slope of the curve) decays with time, indicating that the predominant frequency of the ground acceleration decreases with time. As a measure of the error in fitting to the cumulative number of zero-level up-crossings, we use

$$\varepsilon_\omega = \frac{\int_0^{t_n} \left| \int_0^t \nu(0^+, \tau, \hat{\omega}_0, \hat{\omega}_n, \zeta_f(\tau)) r(\tau)\, d\tau - N(0^+, t) \right| dt}{\int_0^{t_n} N(0^+, t)\, dt} \qquad (37)$$

Values of this measure are listed in Table I for both constant and variable damping models. A similar measure of error in fitting the bandwidth can be defined as the difference between the cumulative numbers of negative maxima and positive minima of the target accelerogram and of the model process, normalized by the cumulative number for the target accelerogram. This measure, denoted ε , is also listed in Table I. Note that this error measure is small only when =0.3 or variable damping is selected.

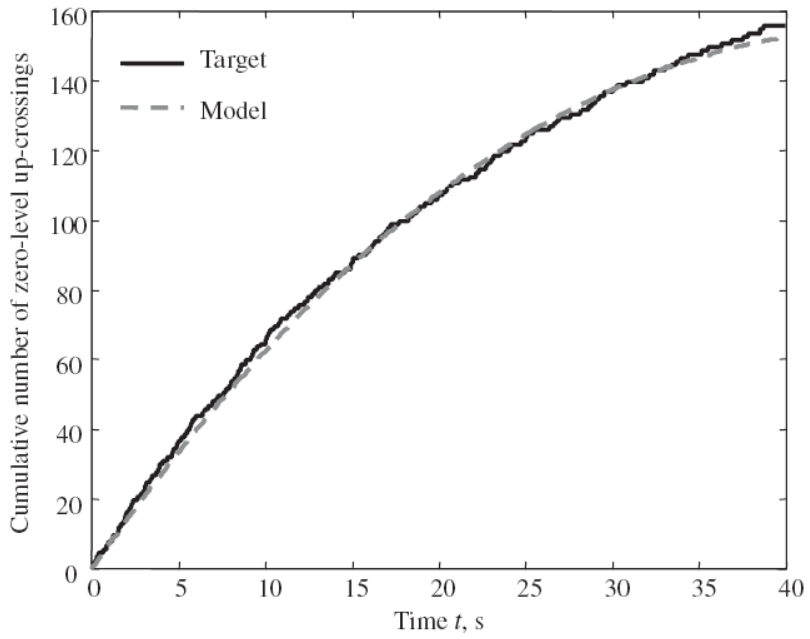

Figure. Cumulative number of zero-level up-crossings in the target accelerogram and fitted model.

3.3 POST-PROCESSING OF SIMULATED MOTION

3.3.1 Description of post-processing

It has been noted in the past that site-based stochastic ground motion models tend to overestimate the structural response at low frequencies. As an example, Figure (a) shows the response spectrum of the Northridge target accelerogram (thick line) together with response spectra of 10 simulated motions with the variable damping model described above (thin lines). It can be seen that, although the simulated spectra match the target spectrum fairly closely for periods shorter than about 2.5 s, at longer periods they all exceed the target spectrum.

The above problem has to do with describing the ground acceleration as a filtered white-noise process. Such a process has a non-zero spectral density at zero frequency and, as a consequence, the integral of the process (the ground velocity or displacement) has infinite spectral density at zero frequency. Because of this property, the variances of the velocity and displacement processes keep on increasing even after the acceleration has vanished. This is contrary to (base-line-corrected) accelerograms, which have zero residual velocity and displacement at the end of the record. To overcome this problem, it is necessary to adjust the low-frequency content of the stochastic model. This is achieved by using a high-pass filter. For this study, we have selected the critically damped oscillator as the high-pass filter. Accordingly, the corrected acceleration record, denoted $\ddot{z}(t)$, is obtained as the solution of the differential equation

$$\ddot{z}(t) + 2\omega_c \dot{z}(t) + \omega_c^2 z(t) = \hat{x}(t) \qquad (38)$$

where ω_c is the frequency of the high-pass filter and $\hat{x}(t)$ is the discretized acceleration process as defined in (32). Due to high damping of the oscillator, it is clear that $z(t)$, $\dot{z}(t)$ and $\ddot{z}(t)$ will

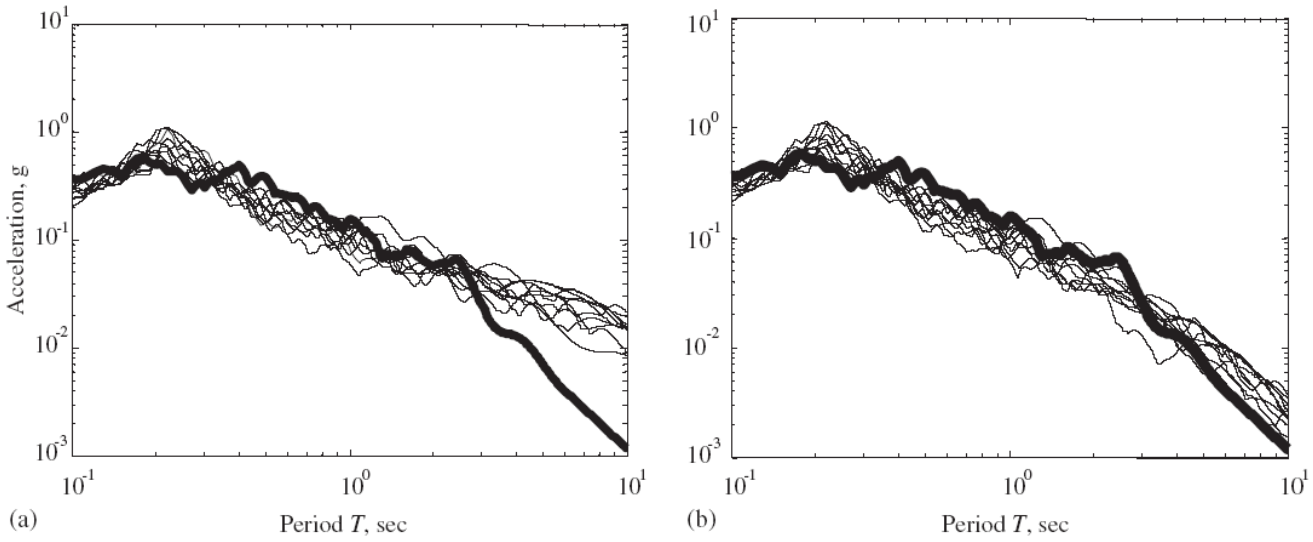

Figure. Pseudo-acceleration response spectra of the target accelerogram (thick line), and 10 realizations of the fitted model (thin lines): (a) before post-processing and (b) after post-processing.

all vanish shortly after the input process $\hat{x}(t)$ has vanished, thus assuring zero residuals for the simulated ground motion. This filter, which was also used by Papadimitriou [24], is motivated by Brune's [9, 11] source model, based on which c, also known as the 'corner frequency,' can be related to the geometry of the seismic source and the shear wave velocity. Most ground motion databases, e.g. http://peer.berkeley.edu/nga/index.html, provide the corner frequency. Note that for stochastic dynamic analysis, the high-pass filter can be included as a part of the structural model so that the discretized form of the input process in (32) can be preserved.

Figure (b) compares the response spectrum of the target accelerogram with the response spectra of the 10 simulated motions, which are post-processed with the filter in (26) with c=0.5_rad/s. It can be seen that the post-processing significantly improves the estimation of spectral values at long periods without affecting the short-period range.

The observed discrepancies between the target and simulated spectra in the short-period range Of Figure 7(b), although not significant, are partly due to the use of a single-degree-of-freedom filter. Such a filter can only characterize a single dominant period in the ground motion. The target recorded ground motion here clearly shows multiple dominant periods. If a closer match is desired, one can select a two-degrees-of-freedom filter, in which case additional parameters will need to be introduced and identified. This is entirely possible with the proposed model but is not pursued in this study.

3.3.2 Adjustment factor for zero-level up-crossings

Consider a stationary filtered white-noise process having the power spectral density $\Phi(\omega) = 1/[(\omega_f^2 - \omega^2)^2 + 4\zeta_f^2\omega_f^2\omega^2]$, which is consistent with the IRF in (20) with time-invariant parameters. The mean zero-level up-crossing rate of the process with the frequencies beyond ω_{max} truncated is given by

$$\nu(0^+, \omega_{max}) = \frac{1}{2\pi}\sqrt{\frac{\int_0^{\omega_{max}} \omega^2\Phi(\omega)\,d\omega}{\int_0^{\omega_{max}} \Phi(\omega)\,d\omega}} \tag{A1}$$

The solid lines in Figure AI show the ratio $r = \nu(0^+, \pi/2\Delta t)/\nu(0^+, \infty)$ as a function of the filter frequency for the damping values $\zeta_f = 0.3$, 0.4, 0.5 and 0.6 and for $\Delta t = 0.01$ and 0.02 s. This ratio

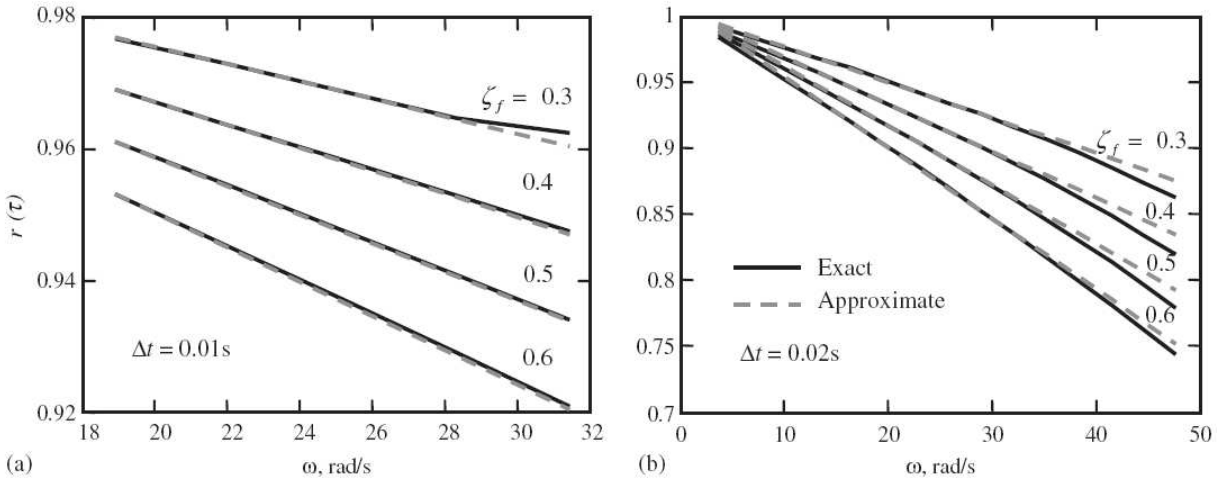

Figure AI. Adjustment factor for undercounting of zero-level up-crossings of a discretized process. represents the undercounting of the zero-level up-crossings, when the process is represented at discrete-time points of interval _*t*. The dotted lines represent the straight-line approximations

$$r(0.01) = 1 - 0.00005(\omega_f + \zeta_f) - 0.00425\omega_f\zeta_f \tag{A2}$$

$$r(0.02) = 1 - 0.01\zeta_f - 0.009\omega_f\zeta_f \tag{A3}$$

It can be seen in Figure AI that representation of a process at discrete-time points can result in undercounting of the zero-level up-crossings by as much as 2–25%, depending on the filter parameters and the time step used.

4. APPLICATIONS

The response of a linear filter with time-varying parameters subjected to a white-noise process is normalized by its standard deviation and is multiplied by a deterministic time-modulating function to obtain the ground acceleration process. Normalization by the standard deviation separates the spectral (achieved by time-variation of the filter parameters) and temporal (achieved by multiplying the process with a time-modulating function) nonstationary characteristics of the process. This model is formulated in the continuous form by (26) and in the discrete form by (32). The discrete form is ideal for digital simulation and for use in nonlinear random vibration analysis by the tail-equivalent linearization method. The model is completely defined by the form of the filter IRF and the modulating function and their parameters. Suggested models for the IRF and the modulating function and their parameters are provided. The stochastic model may have as few as six parameters that control the statistical characteristics of the ground motion. The simulated acceleration process according to (32) is then high-pass filtered in accordance with (38) to assure zero residual velocity and displacement, as well as to produce reliable response spectral values at long periods. Figure illustrates the steps involved in simulating a single ground acceleration time-history for a given set of model parameters.

For specified parameters of the modulating function and the filter IRF, sample realizations of the proposed stochastic ground motion model are generated by the use of (32). This requires generation of the standard normal random variables ui , i =1, . . . ,n, and their multiplication by the functions $si\ (t)$, which are computed according to (33). The resulting motion is then postprocessed as described in the previous section. Figure 8 shows the target Northridge accelerogram together with two sample realizations simulated using the fitted stochastic model. These simulated ground motions have evolutionary statistical characteristics, i.e. time-varying intensity, predominant frequency and bandwidth, which are similar to those of the target accelerogram. Hence, together with the target accelerogram, they can be considered as realizations of a stochastic ground motion having the characteristics of the earthquake and site, which produced the target motion. Such an ensemble of ground motions would be appropriate for design or assessment of a structure for that particular earthquake. However, in the broader context of PBEE design and analysis, an ensemble of ground motions that represents all possible earthquakes at a site is of interest. The proposed model can be used to generate such an ensemble as described below

Suppose we fit the model to a large ensemble of accelerograms with known earthquake and recording site characteristics, e.g. the earthquake magnitude, distance, faulting type, depth to bedrock, site

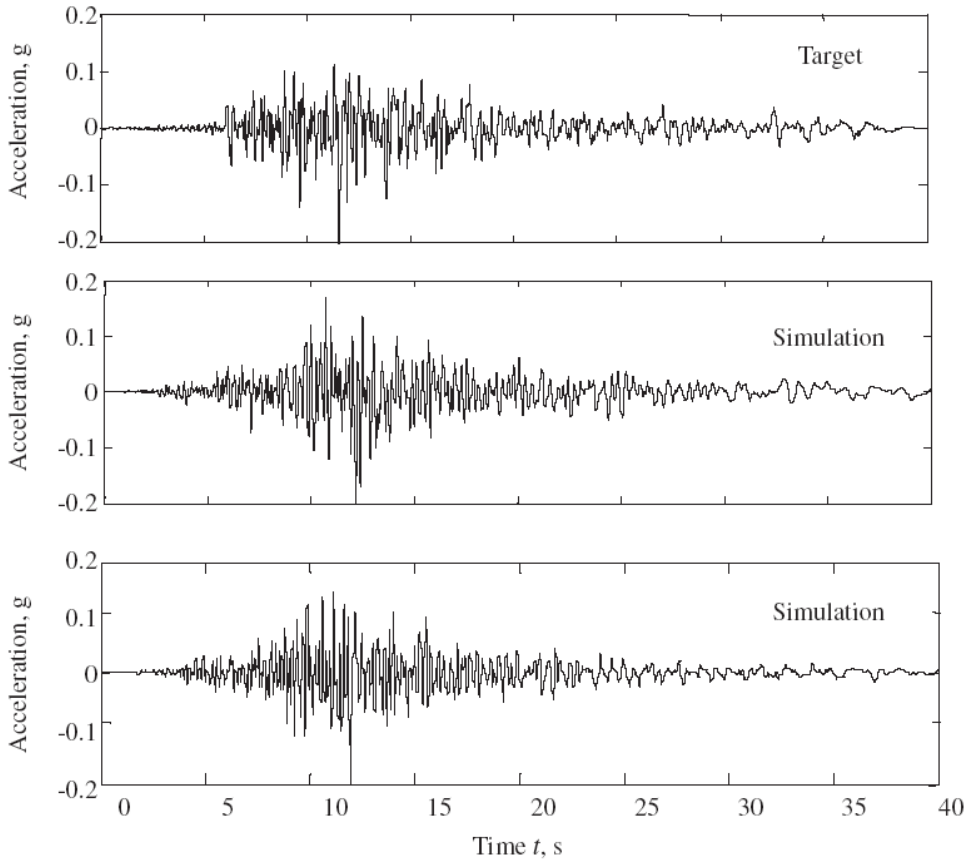

Figure. Target accelerogram and two simulations using the fitted model.

.

shear wave velocity. The result will be a database of the model parameters for the given values of the earthquake and site characteristics. By regressing the former against the latter, one can develop predictive relations for the model parameters in terms of the earthquake and site characteristics (similar to attenuation laws). Let $\boldsymbol{\theta}=\mathbf{g}(\mathbf{x})+\boldsymbol{\varepsilon}$ denote the set of relations between the model parameters, $\boldsymbol{\theta}$, and the earthquake and site characteristic variables, $\mathbf{x}$, with $\boldsymbol{\varepsilon}$ denoting the zero-mean regression errors. For a given set of earthquake variables $\mathbf{x}$, an 'average' ground motion is generated using the mean model parameters $\boldsymbol{\theta}=\mathbf{g}(\mathbf{x})$. An entire suit of motions for given $\mathbf{x}$ can be generated by randomizing $\boldsymbol{\varepsilon}$ and computing the corresponding values of the model parameters. This process can be repeated for different sets of earthquake and site characteristics $\mathbf{x}$, thus generating an entire suite of artificial ground motions for the PBEE design and analysis. Because of the fact that the parameters of the proposed model are directly related to the physical characteristics of the ground motion (i.e. intensity, predominant frequency and bandwidth) it is likely that the regressions with earthquake and site characteristics will produce good predictive models. This study is currently underway.

5. NUMERICAL STUDY

5.1 Numerical Examples

Example 1: The matlab program has been given the value as follows:

INPUT DATA:

Damping ratio(ζ) =0.3,

Filter frequency at time t_0 ($\omega_{0)}$= 39.7 ,

Filter frequency at time t_n ($\omega_{n)}$= 4.68,

Initial time (t_0) = 0.0004 sec.,

Total time duration (t_n) = 40 sec.,

MODULATING FUNCTION PARAMETERS :

Start of the strong motion phase(T_1) =12.2sec.,

End of the strong motion phase(T_2) =12.2sec.,

R.M.S value of the function = 0.0744g,

α (shape the decaying end of the function) =0.413,

β (shape the decaying end of the function) =0.552,

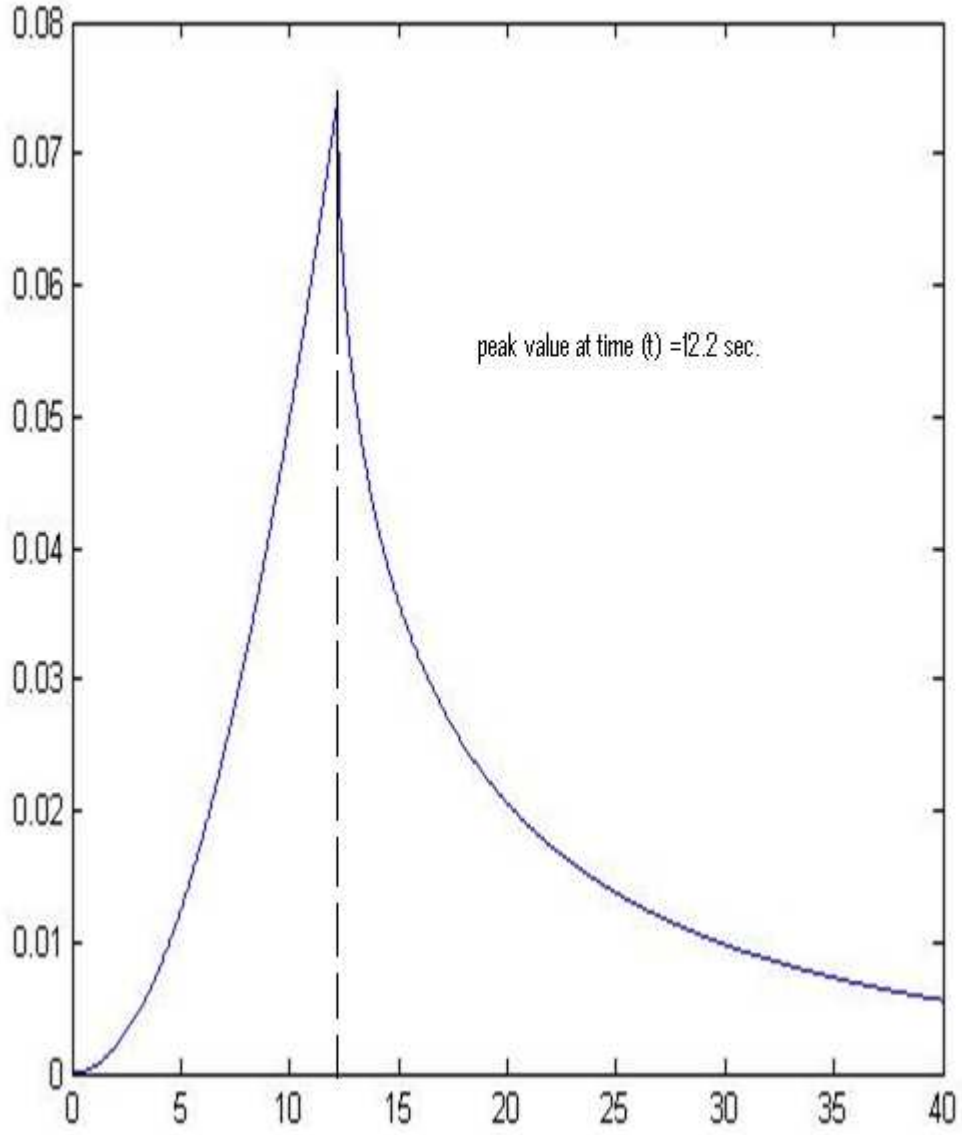

TIME (IN SEC)

Y AXIS REPRESENTS THE MODULATING FUNCTION

The above graph shows the variation of modulating function with respect to time.

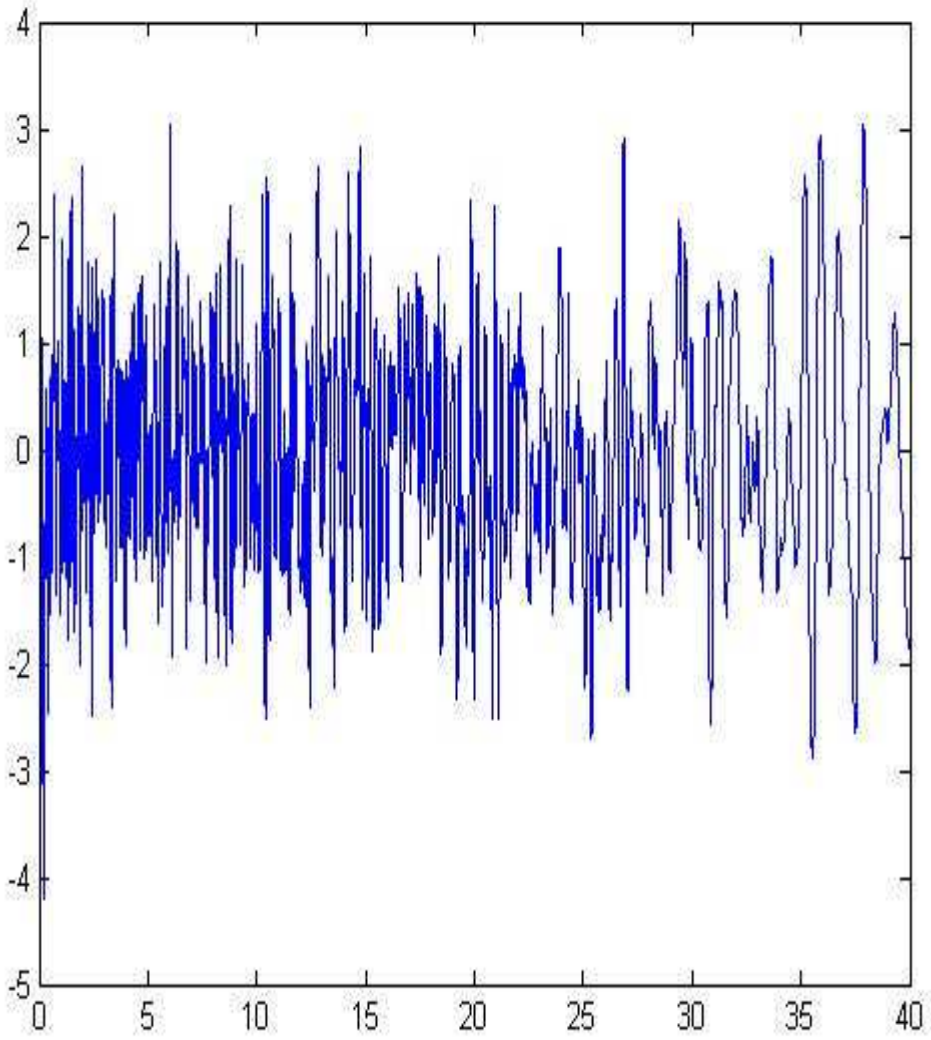

TIME (IN SEC)

Y AXIS REPRESENTS THE ACCELERATION

The above graph shows the variation of acceration Vs time in the unmodulated process.

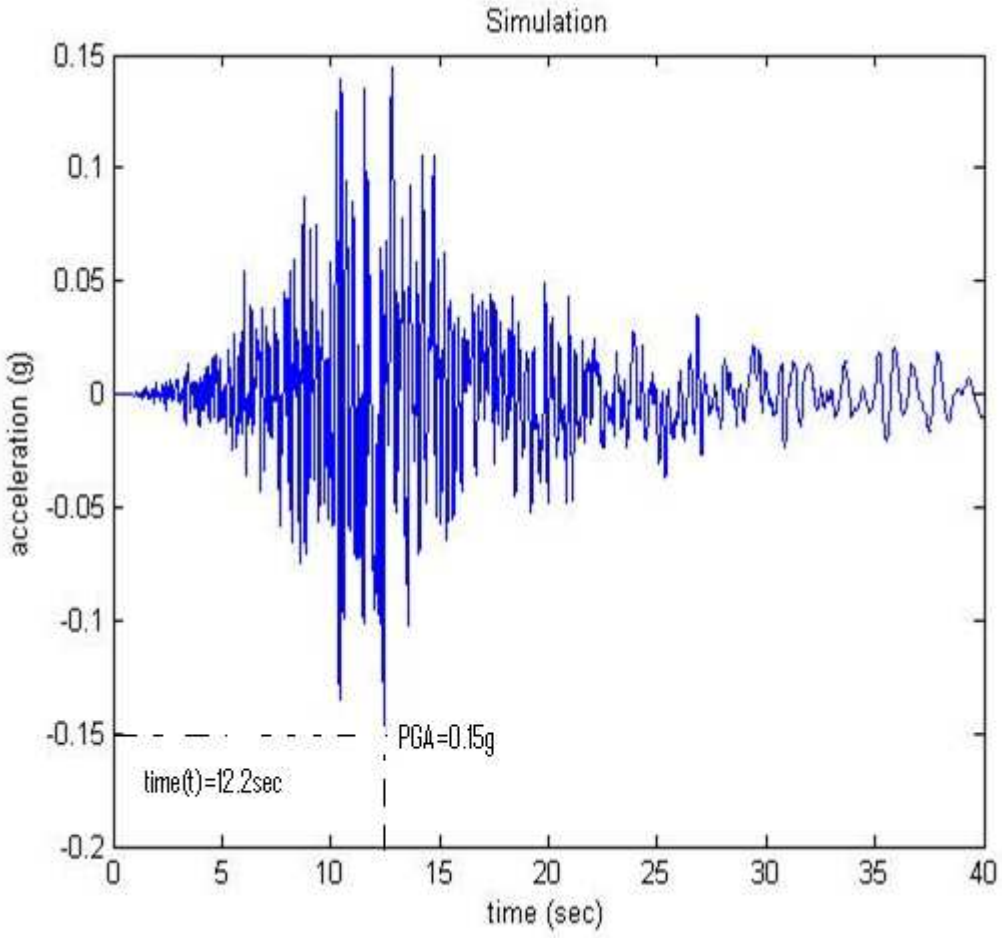

The above final graph shows the variation of acceleration Vs time in the modulated process.

Example 2: The matlab program has been given the value as follows:

INPUT DATA:

Damping ratio(ζ) =0.2,

Filter frequency at time t_0 ($\omega_{0)}$= 40.8,

Filter frequency at time t_n ($\omega_{n)}$= 4.16,

Initial time (t_0) = 0.0004 sec.,

Total time duration (t_n) = 40 sec.,

MODULATING FUNCTION PARAMETERS :

Start of the strong motion phase (T_1) =12.2sec.,

End of the strong motion phase (T_2) =12.2sec.,

R.M.S value of the function = 0.0744g,

α (shape the decaying end of the function) =0.413,

β (shape the decaying end of the function) =0.552,

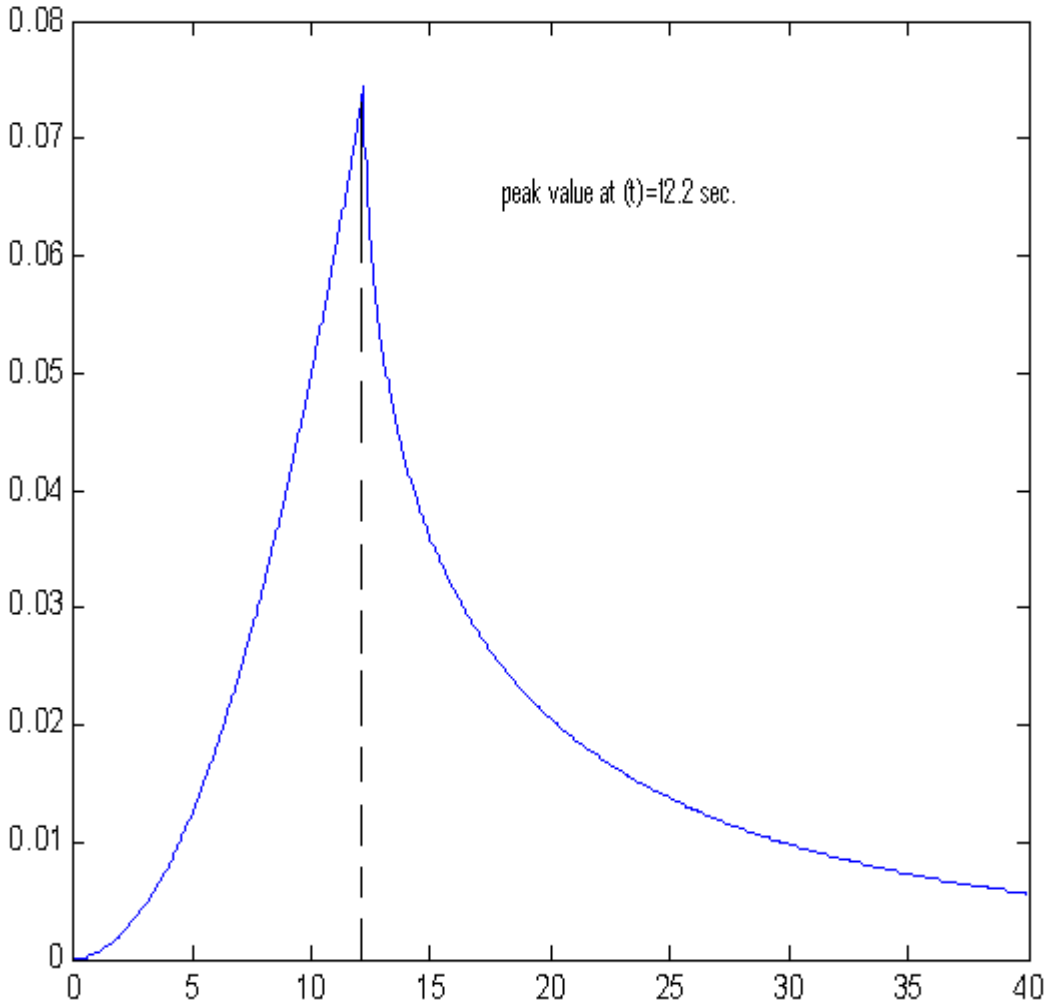

TIME (IN SEC)

Y AXIS REPRESENTS THE MODULATING FUNCTION

The above graph shows the variation of modulating function with respect to time.

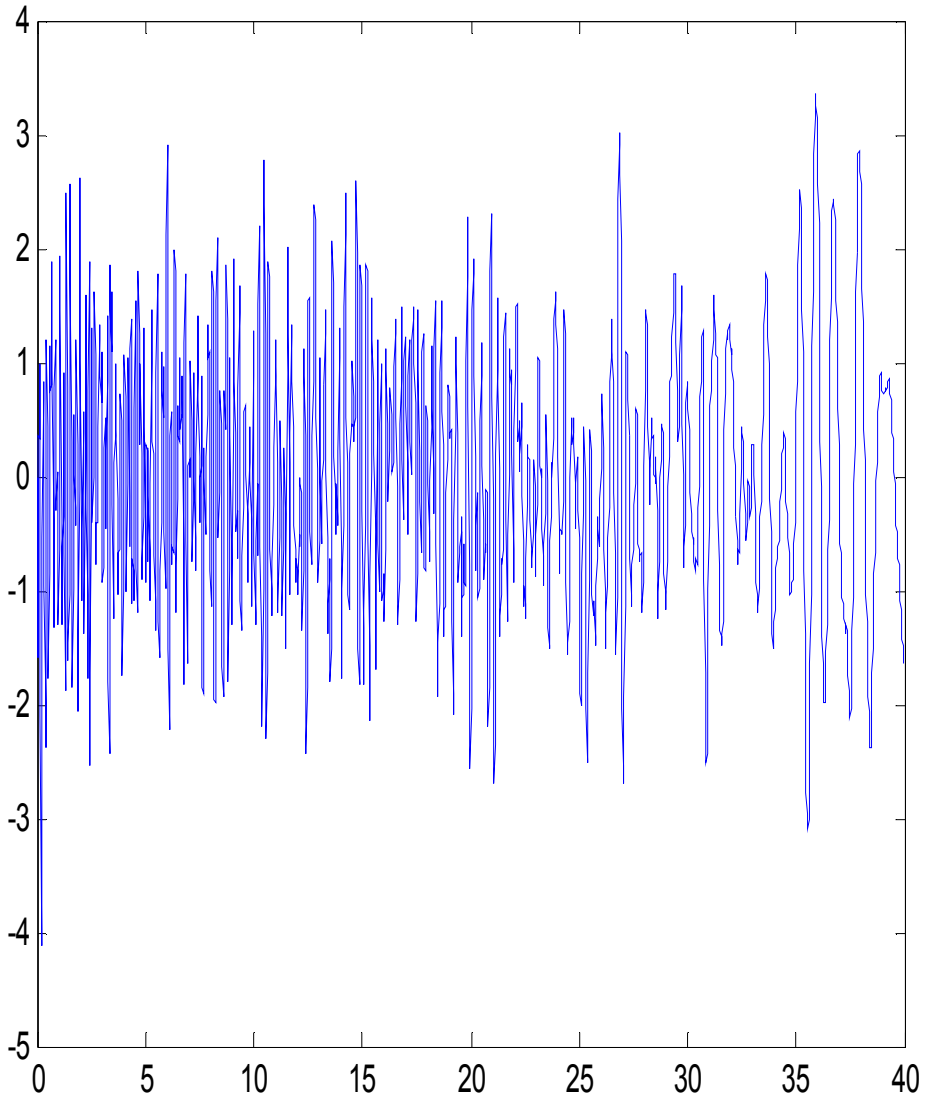

TIME (IN SEC)

Y AXIS REPRESENTS THE ACCELERATION

The above graph shows the variation of acceleration Vs time in the unmodulated process.

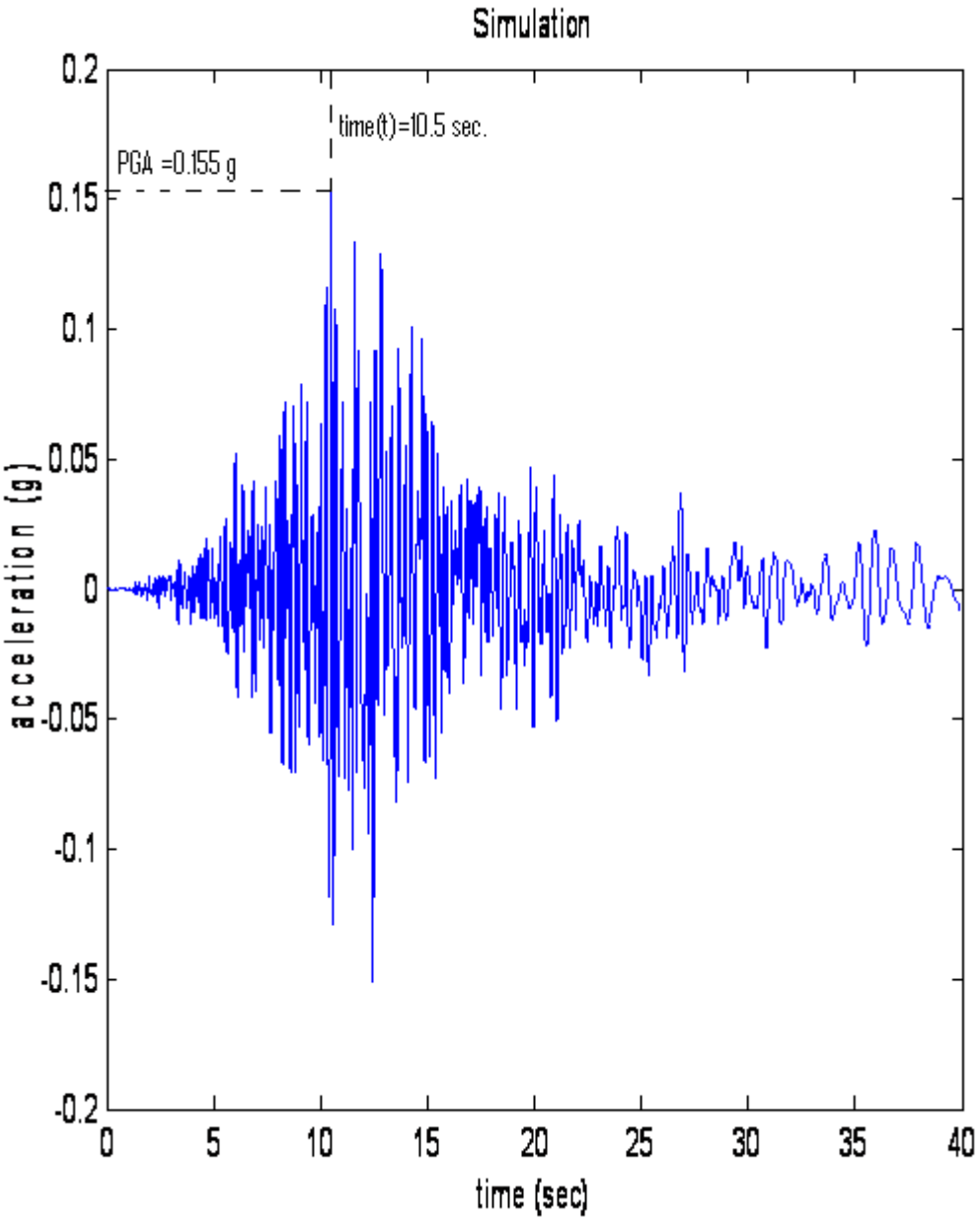

The above final graph shows the variation of acceleration Vs time in the modulated process.

Example 3: The matlab program has been given the value as follows:

INPUT DATA:

Damping ratio(ζ) =0.4,

Filter frequency at time t_0 ($\omega_{0)}$= 38.6,

Filter frequency at time t_n ($\omega_{n)}$= 4.49,

Initial time (t_0) = 0.0004 sec.,

Total time duration (t_n) = 40 sec.,

MODULATING FUNCTION PARAMETERS :

Start of the strong motion phase (T_1) =12.2sec.,

End of the strong motion phase (T_2) =12.2sec.,

R.M.S value of the function = 0.0744g,

α (shape the decaying end of the function) =0.413,

β (shape the decaying end of the function) =0.552,

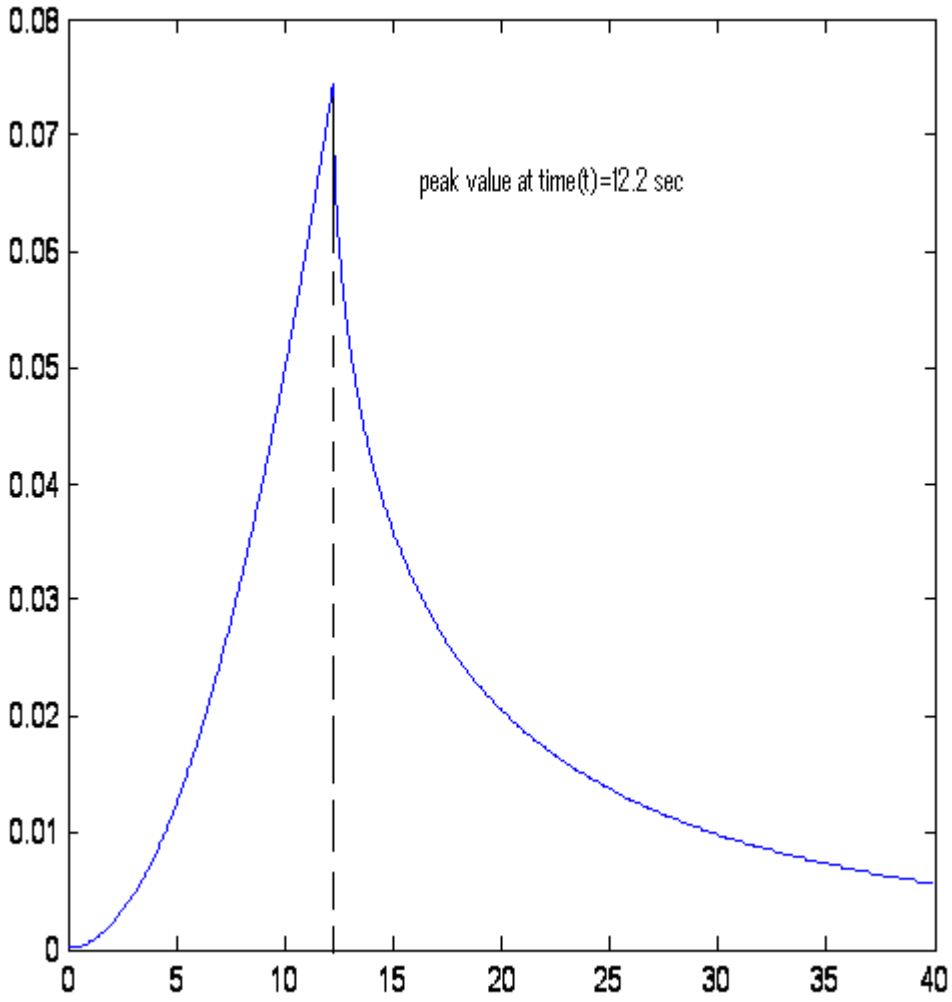

TIME (IN SEC)

Y AXIS REPRESENTS THE MODULATING FUNCTION

The above graph shows the variation of modulating function with respect to time.

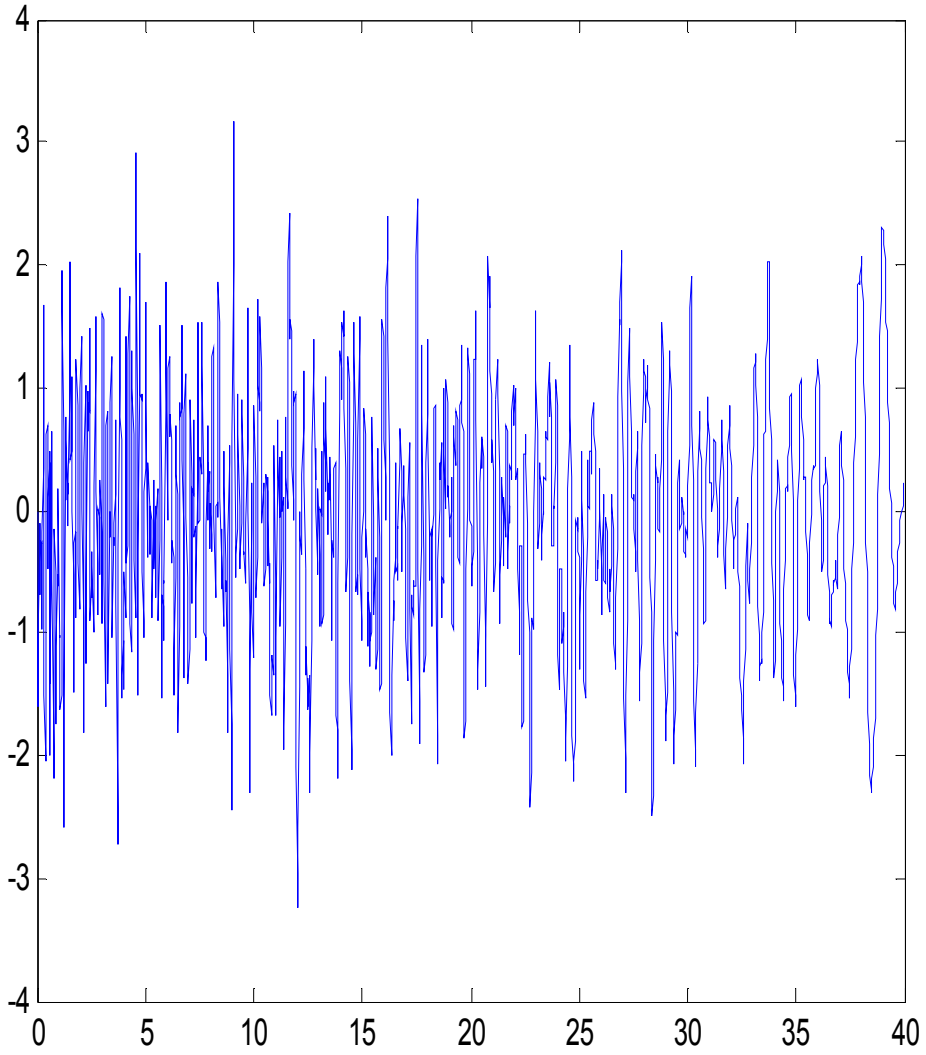

TIME (IN SEC)

Y AXIS REPRESENTS THE ACCELERATION

The above graph shows the variation of acceration Vs time in the unmodulated process.

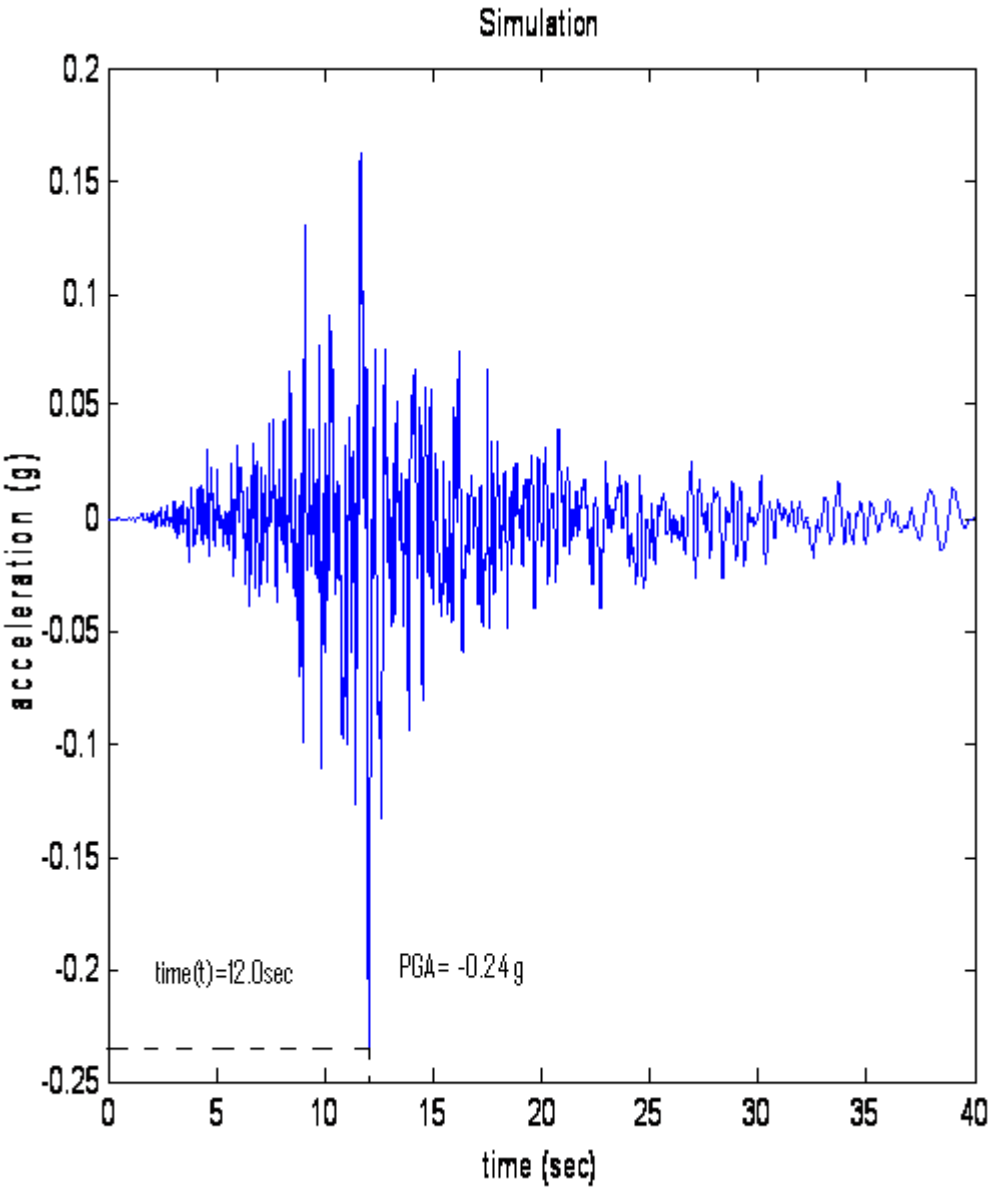

The above final graph shows the variation of acceleration Vs time in the modulated process.

5.2 COMPARISON OF TARGET AND SIMULATED ACCELEROGRAMS

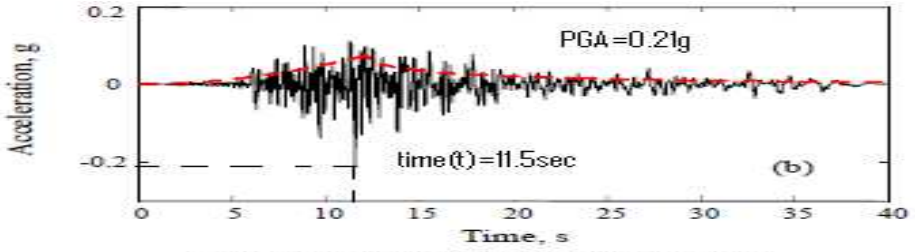

TARGET ACCELEROGRAM WITH CORRESPONDING
MODULATING FUNCTION SUPERIMPOSED (RED LINE)

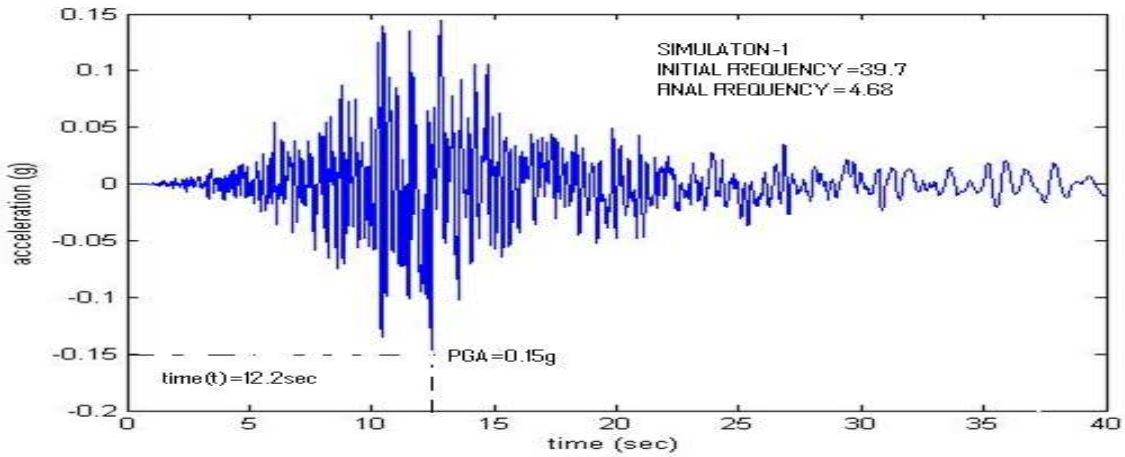

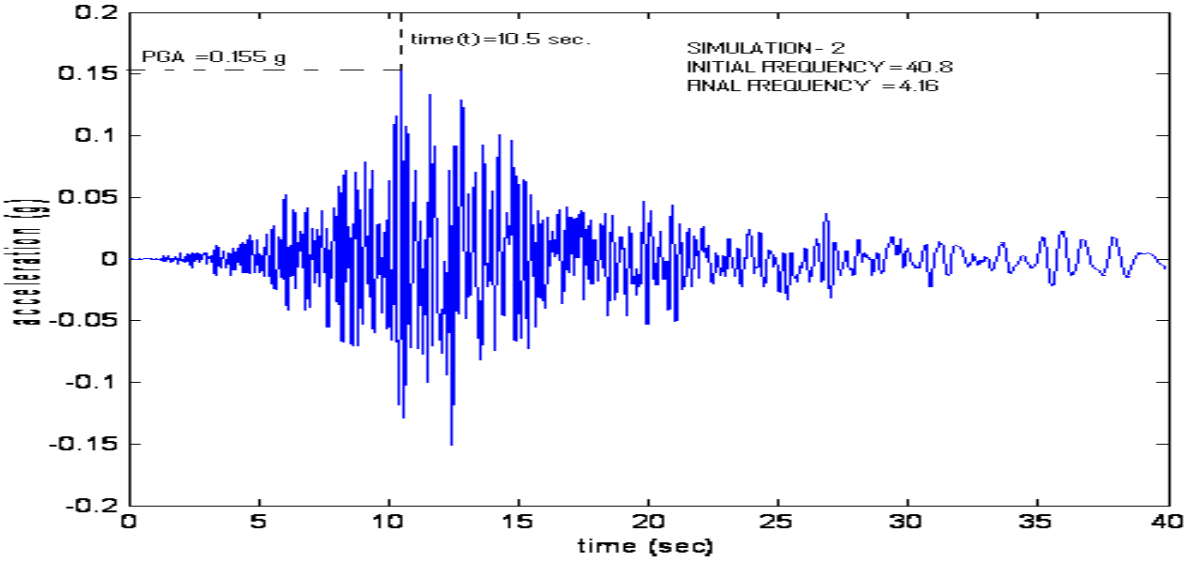

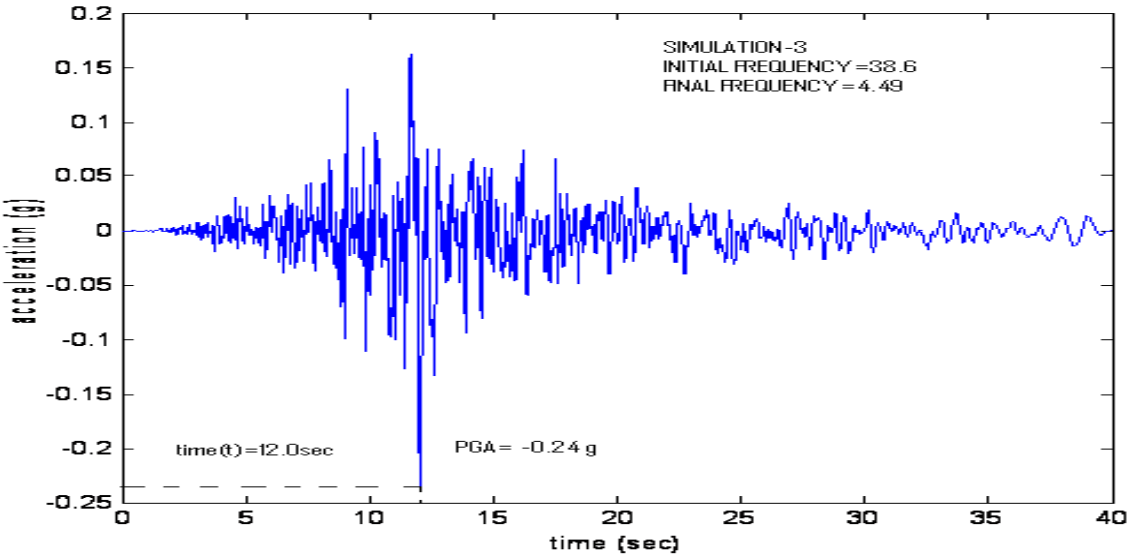
SIMULATION-3
INITIAL FREQUENCY =38.6
FINAL FREQUENCY = 4.49
time(t)=12.0sec
PGA= -0.24 g
acceleration (g)
time (sec)
0.2
0.15
0.1
0.05
0
-0.05
-0.1
-0.15
-0.2
-0.25
0
5
10
15
20
25
30
35
40

6. CONCLUSIONS & ANNEXURE

6.1 Conclusion

A fully nonstationary stochastic model to describe earthquake ground motions is developed. The model is based on the modulation of the response of a linear filter with time-varying characteristics to a discretized white-noise excitation. The proposed model has a number of important advantages. One significant advantage is that the temporal and spectral nonstationary characteristics of the process are separate, facilitating the identification and interpretation of the model parameters. Specifically, the modulating function characterizes the variation of the intensity in time, whereas the time-varying filter parameters define the evolving frequency content of the process. The model parameters are estimated by fitting to selected statistical characteristics of a target accelerogram. There is no need for sophisticated processing of the recorded motion such as Fourier analysis or estimation of evolutionary power spectral density. Instead, the model fitting requires computation of the cumulative energy and the cumulative counts of zero-level up-crossings, negative maxima and positive minima of the accelerogram.

The model can be used to simulate artificial ground motions having statistical characteristics similar to those of the target accelerogram. The simulation requires little more than generation of standard normal random variables, their multiplication with deterministic time functions, and post-processing through a high-pass filter to correct the long-period content of the spectrum. Furthermore, the model is of a form, which facilitates the nonlinear random vibration analysis by TELM.

An example application using an accelerogram of the 1994 Northridge earthquake as the target motion is described in detail. The example demonstrates the effectiveness of the proposed parameter estimation method and the faithfulness of the model in reproducing realizations with statistical characteristics similar to those of the target motion. By fitting to different recorded ground motions, one can generate a library of simulated motions with specified earthquake and site characteristics for use in performance-based earthquake engineering analysis.

6.2.ANNEXURE

6.2.1 Program listing

Stochastic model has been developed in the matlab software. The following is the input file of the program:

1*********!**********q_Iq2_B.m *********

```
switch Type


    case 'piece-wise'


for r=1:n
    tr=(r-1)*deltat;
    if tr<T0
        q(r)=0;
    else
        if tr<T1
            q(r)=((tr-T0)/(T1-T0))^2;
        else
            if tr<T2
                q(r)=1;
            else
                q(r)=exp(-S*((tr-T2)^B));
            end
        end
    end
end
```

```
q=q*D;
q2_Integ(1)=0;
for r=2:n
    q2_Integ(r)=q2_Integ(r-1)+q(r)^2;
end
q2_Integ=q2_Integ*deltat;
```

2**********SampleSiml.m**********

```
% Created by vivek kumar pankaj
% Last update: 12/21/2011
% Simulate a ground motion given parameters according to 2008paper
% Accompanied by: q_Iq2_B.m  simf.m

%% Simulation (n=tn*tdeltat/deltat)
n=2000;
deltat=0.02;

%% Specify the type of the deterministic modulating function q(t)
Type='piece-wise';
T0=0.0004;
T1=12.2;
T2=12.2;
D=0.0744;
S=0.413;
B=0.552;
q_Iq2_B %%this script creates functions q(t) and q2_Integ(t)
```

```
figure
plot(0:deltat:(n-1)*deltat,q)

%% Simulate the filter
a=39.7;
b=(a-4.68)/((n-1)*deltat);
c=0.3;
figure
f=simf(a,b,c,n,deltat);  %% Generates the unmodulated process

%% final form of the realization
F=q.*f;
figure
plot(0:deltat:(n-1)*deltat,F)
xlabel('time (sec)')
ylabel('acceleration (g)')
title('Simulation')
```

**********simf.m**********

```
function f=simf(a,b,c,n,deltat)
%%% Generates the unmodulated simulation

for r=1:n
    t(r)=(r-1)*deltat;
end

f=zeros(1,n);
```

```
C=zeros(1,n);
zeta=c;

%% Find the scale parameter, C vector
for j=1:n
    tj=t(j);
    omega=a-b*tj;
    omegaD=omega*sqrt(1-zeta^2);
    for i=1:n
        ti=t(1)+(i-1)*deltat;
        if ti>=tj
            hf=-(omega/sqrt(1-zeta^2))*exp(-zeta*omega*(ti-
tj))*sin(omegaD*(ti-tj));
            Cj(i)=hf.^2;
        else
            Cj(i)=0;
        end
    end
    C = C + Cj;
end
C=C.^(.5);
C(1)=.1;

%% Generate the Sj vectors:
for j=1:n
    tj=t(j);
    uj=randn(1);
```

```
    cj=C(j);
    omega=a-b*tj;
    omegaD=omega*sqrt(1-zeta^2);
    for i=1:n
        ti=t(1)+(i-1)*deltat;
        if ti>=tj
            hf=-(omega/sqrt(1-zeta^2))*exp(-zeta*omega*(ti-
tj))*sin(omegaD*(ti-tj));
            Sj(i)=hf;
        else
            Sj(i)=0;
        end
    end
    f = f + Sj*uj;
end

%% Scale f to normalize its standard deviation
f=f./C;
plot(t,f)
```

7. REFERENCES

JOURNALS

1. Bolotin VV. Statistical theory of the aseismic design of structures. *Proceedings of the 2nd World Conference on Earthquake Engineering*, vol. II, Tokyo and Kyoto, Japan, 1960; 1365–1374.
2. Cornell CA. Stochastic process models in structural engineering. *Technical Report No. 34*, Department of Civil Engineering, Stanford University, Stanford, CA, 1960.
3. Housner GW, Jennings PC. Generation of artificial earthquakes. *Journal of Engineering Mechanics Division* (ASCE) 1964; **90**:113–150.
4. Lin YK. Nonstationary excitation and response in linear systems treated as sequences of random pulses. *Journal of the Acoustical Society of America* 1965; **38**:453–460.
5. Shinozuka M, Sato Y. Simulation of nonstationary random process. *Journal of Engineering Mechanics* (ASCE) 1967; **93**:11–40.
6. Amin M, Ang AHS. Nonstationary stochastic model of earthquake motions. *Journal of Engineering Mechanics Division* (ASCE) 1968; **94**:559–583.
7. Iyengar RN, Iyengar KTS. A nonstationary random process model for earthquake accelerograms. *Bulletin of the Seismological Society of America* 1969; **59**:1163–1188.
8. Liu SC. Synthesis of stochastic representations of ground motions. *The Bell Systems Technical Journal* 1970; **49**:521–541.
9. Brune JN. Tectonic stress and the spectra of seismic shear waves from earthquakes. *Journal of Geophysical Research* 1970; **75**:4997–5009.
10. Ruiz P, Penzien J. Stochastic seismic response of structures. *Journal of Engineering Mechanics* (ASCE) 1971; **97**:441–456 .
11. Brune JN. Correction. *Journal of Geophysical Research* 1971; **76**:5002.
12. Saragoni GR, Hart GC. Simulation of artificial earthquakes. *Earthquake Engineering and Structural Dynamics* 1974; **2**:249–267.
13. Jurkevics A, Ulrych TJ. Representing and simulating strong ground motion. *Bulletin of the Seismological Society of America* 1978; **68**:781–801.
14. Hoshiya M, Hasgur Z. AR and MA models of nonstationary ground motion. *Bulletin of the International Institute of Seismology and Earthquake Engineering* 1978; **16**:55–68.
15. Ahmadi G. Generation of artificial time-histories compatible with given response spectra—a review. *Solid Mechanics Archives* 1979; **4**:207–239.
16. Polhemus NW, Cakmak AS. Simulation of earthquake ground motions using autoregressive moving average (ARMA) models. *Earthquake Engineering and Structural Dynamics* 1981; **9**:343–354.

17. Chang MK, Kwiatkowski JW, Nau RF, Oliver RM, Pister KS. ARMA models for earthquake ground motions. *Earthquake Engineering and Structural Dynamics* 1982; **10**:651–662.
18. Lin YK. On random pulse train and its evolutionary spectral representation. *Probabilistic Engineering Mechanics* 1986; **1**:219–223.
19. Zerva A. Seismic source mechanisms and ground motion models, review paper. *Probabilistic Engineering Mechanics* 1988; **3**:64–74.
20. Shinozuka M, Deodatis G. Stochastic process models for earthquake ground motion. *Probabilistic Engineering Mechanics* 1988; **3**:114–123.
21. Kozin F. Autoregressive moving average models of earthquake records. *Probabilistic Engineering Mechanics* 1988; **3**:58–63.
22. Der Kiureghian A, Crempien J. An evolutionary model for earthquake ground motion. *Structural Safety* 1989; **6**:235–246.
23. Yeh CH, Wen YK. Modeling of nonstationary ground motion and analysis of inelastic structural response. *Structural Safety* 1990; **8**:281–298.
24. Papadimitriou K. Stochastic characterization of strong ground motion and application to structural response. *Report No. EERL 90-03*, Earthquake Engineering Research Laboratory, California Institute of Technology, Pasadena, CA, 1990.
25. Conte JP, Pister KS, Mahin SA. Nonstationary ARMA modeling of seismic motions. *Soil Dynamics and Earthquake Engineering* 1992; **11**:411–426.
26. Conte JP, Peng BF. Fully nonstationary analytical earthquake ground-motion model. *Journal of Engineering Mechanics* (ASCE) 1997; **12**:15–24.
27. Der Kiureghian A. The geometry of random vibrations and solutions by FORM and SORM. *Probabilistic Engineering Mechanics* 2000; **15**:81–90.
28. Vamvatsikos D, Cornell CA. Incremental dynamic analysis. *Earthquake Engineering and Structural Dynamics* 2002; **31**:491–514.
29. Mobarakeh AA, Rofooei FR, Ahmadi G. Simulation of earthquake records using time-varying ARMA *(*2,1*)* model. *Probabilistic Engineering Mechanics* 2002; **17**:15–34.
30. Bozorgnia Y, Bertero VV. *Earthquake Engineering*: *From Engineering Seismology to Performance-based Engineering*. CRC Press: Boca Raton, FL, 2004.
31. Wen YK, Gu P. Description and simulation of nonstationary processes based on Hilbert spectra. *Journal of Engineering Mechanics* (ASCE) 2004; **130**:942–951.
32. Lutes LD, Sarkani S. *Random Vibrations*: *Analysis of Structural and Mechanical Systems*. Elsevier Butterworth- Heinemann: Burlington, MA, 2004.

33. Fujimura K, Der Kiureghian A. Tail-equivalent linearization method for nonlinear random vibration. *ProbabilisticEngineering Mechanics* 2007; **22**:63–76.

BOOKS

1. Applications of random vibrations .*N.C.Nigam & S. Narayanan*.
2. Random vibration in mechanical systems. *Stephen H.Crandall & William D. Mark*